Title
Large-scale distribution of CH_4in the western North Pacific: Sources and transport from the Asian continent

Journal
Journal of Geophysical Research, 108(D20)

ISSN
0148-0227

Author
Bartlett, Karen B

Publication Date
2003

DOI
10.1029/2002jd003076

Large-scale distribution of CH_4 in the western North Pacific: Sources and transport from the Asian continent

Karen B. Bartlett,[1] Glen W. Sachse,[2] Thomas Slate,[3] Charles Harward,[4] and Donald R. Blake[5]

Received 24 October 2002; revised 14 May 2003; accepted 30 May 2003; published 23 September 2003.

[1] Methane (CH_4) mixing ratios in the northern Pacific Basin were sampled from two aircraft during the TRACE-P mission (Transport and Chemical Evolution over the Pacific) from late February through early April 2001 using a tunable diode laser system. Described in more detail by *Jacob et al.* [2003], the mission was designed to characterize Asian outflow to the Pacific, determine its chemical evolution, and assess changes to the atmosphere resulting from the rapid industrialization and increased energy usage on the Asian continent. The high-resolution, high-precision data set of roughly 13,800 CH_4 measurements ranged between 1602 ppbv in stratospherically influenced air and 2149 ppbv in highly polluted air. Overall, CH_4 mixing ratios were highly correlated with a variety of other trace gases characteristic of a mix of anthropogenic industrial and combustion sources and were strikingly correlated with ethane (C_2H_6) in particular. Averages with latitude in the near-surface (0–2 km) show that CH_4 was elevated well above background levels north of 15°N close to the Asian continent. In the central and eastern Pacific, levels of CH_4 were lower as continental inputs were mixed horizontally and vertically during transport. Overall, the correlation between CH_4 and other hydrocarbons such as ethane (C_2H_6), ethyne (C_2H_2), and propane (C_3H_8) as well as the urban/industrial tracer perchloroethene (C_2Cl_4), suggests that for CH_4 colocated sources such as landfills, wastewater treatment, and fossil fuel use associated with urban areas dominate regional inputs at this time. Comparisons between measurements made during TRACE-P and those of PEM-West B, flown during roughly the same time of year and under a similar meteorological setting 7 years earlier, suggest that although the TRACE-P CH_4 observations are higher, the changes are not significantly greater than the increases seen in background air over this time interval. *INDEX TERMS:* 0345 Atmospheric Composition and Structure: Pollution—urban and regional (0305); 0365 Atmospheric Composition and Structure: Troposphere—composition and chemistry; 0368 Atmospheric Composition and Structure: Troposphere—constituent transport and chemistry; 1610 Global Change: Atmosphere (0315, 0325); *KEYWORDS:* methane, TRACE-P, Pacific Basin

Citation: Bartlett, K. B., G. W. Sachse, T. Slate, C. Harward, and D. R. Blake, Large-scale distribution of CH_4 in the western North Pacific: Sources and transport from the Asian continent, *J. Geophys. Res.*, *108*(D20), 8807, doi:10.1029/2002JD003076, 2003.

1. Introduction

[2] The increasing industrialization occurring throughout the Asian continent has spurred a series of research efforts over the past decade, attempting to assess how these quantitative and qualitative changes in emissions have affected the global atmosphere. These efforts have included NASA's PEM West A and B missions, flown in 1991 and 1994, respectively, which examined the effects of seasonal differences in meteorology, transport, and source strengths on air quality over the Pacific Basin (see *Hoell et al.* [1997] for summary). The most recent research program conducted over this region is that of TRACE-P (Transport and Chemical Evolution over the Pacific), focused on improving our understanding of how outflow from the Asian continent affects the composition of the atmosphere over the Pacific and assessing the changes that have occurred since PEM West, as rapid industrialization and increased energy usage have continued [*Streets et al.*, 2003]. TRACE-P is the latest aircraft mission flown by NASA as part of its Global Tropospheric Experiment (GTE) which has undertaken to both characterize the natural processes controlling the chemistry of the troposphere and to determine how anthropogenic perturbations have affected this chemistry. Building on the earlier PEM-West missions, TRACE-P was flown from 23 February–9 April of 2001, when continental

[1]Institute for the Study of Earth, Oceans, and Space, University of New Hampshire, Durham, New Hampshire, USA.
[2]NASA Langley Research Center, Hampton, Virginia, USA.
[3]Swales Aerospace, Hampton, Virginia, USA.
[4]Science Applications International Corporation, Hampton, Virginia, USA.
[5]Department of Chemistry, University of California, Irvine, Irvine, California, USA.

0148-0227/03/2002JD003076

outflow to the Pacific Basin was expected to be near its peak due to strong westerly transport and active convection over Asia [*Merrill et al.*, 1997]. Matching the timing of TRACE-P to that of PEM-West B also provides an opportunity to compare results under similar meteorological conditions and to focus on possible changes in emissions over the intervening 7 years.

[3] The TRACE-P mission used two NASA aircraft, a DC-8 with a maximum sampling altitude of about 12 km and a P-3B with a maximum sampling altitude of about 7 km. Samples were taken most intensively between roughly 20°N and 40°N. Flight tracks and a description of the instrumentation and its characteristics can be found in the work of *Jacob et al.* [2003]. Sampling was conducted later by several weeks than that during PEM-West B (hereafter noted as PWB), which was flown 25 January–16 March 1994. As detailed by *Fuelberg et al.* [2003], TRACE-P was flown during the transition between air flows characteristic of winter to those of spring. The ITCZ (Intertropical Convergence Zone) was not well developed during the mission and the Japan Jet, located at about 35°N and extending west back to Africa, was relatively strong, as is typical for this time of year. Widespread areas of precipitation covered the middle latitudes of the North Pacific Basin during the mission, some in association with lightning and the rapid vertical transport characteristic of deep convection. TRACE-P sampling occurred during neutral to weak La Nina conditions [*Fuelberg et al.*, 2003] and flow patterns and precipitation appear to be quite similar to the meteorological conditions observed during PWB.

[4] Methane (CH_4) is the most abundant atmospheric hydrocarbon, with a lifetime of roughly 9 years [*Prinn et al.*, 1995]. Although atmospheric levels of CH_4 are much lower than CO_2, the fact that CH_4 absorbs outgoing radiation more efficiently means that change in its atmospheric burden significantly impacts climate change. Methane plays important radiative and chemical roles in both the troposphere and stratosphere and has undergone a variable and poorly understood increase over the last several hundred years [*Etheridge et al.*, 1998; *Dlugokencky et al.*, 1994, 1998; *Gupta et al.*, 1996; *Francey et al.*, 1999; *Bräunlich et al.*, 2001]. Sources of CH_4 are both natural and anthropogenic and are linked to climate variables as well as human populations and energy usage. Ongoing changes occurring over the Asian continent in population, land use, and the sources and quantity of energy used will significantly impact the release of CH_4 [*Streets et al.*, 2001].

[5] TRACE-P was flown in the northern Asian spring. Methane emissions from natural wetlands as well as rice paddies, calculated to be the single largest anthropogenically controlled source in this region [*Streets et al.*, 2001], are therefore expected to be near seasonal lows. Inverse modeling of atmospheric concentrations confirm this generalization and suggest that emissions from natural wetlands in southeast Asia result in only minor increases in CH_4 levels during the spring [*Houweling et al.*, 2000]. Temperatures and rainfall, major controls on emissions from wetlands, are relatively low during this period and the seasonal planting of rice is just commencing [*Matthews et al.*, 1991; *Yao et al.*, 1996; *Khalil et al.*, 1998]. In China for example, *Yao et al.* [1996] estimate that 95% of the annual flux of CH_4 from rice paddies occurs between April and October, with peak emissions in June. Emissions of CH_4 would therefore expected to be dominated by urban and industrial sources such as landfills, wastewater treatment, and fuel usage. In more rural areas, CH_4 produced during enteric fermentation by ruminants such as cattle makes a significant contribution. These sources would not be expected to show large seasonal changes. Incomplete combustion during biofuel and biomass burning can also release significant amounts of CH_4. Biomass burning varies seasonally and should be decreasing from its winter seasonal maximum [*Hao and Liu*, 1994; *Cooke et al.*, 1996; *Randriambelo et al.*, 2000]. Biofuel burning, largely for cooking or energy uses [*Brocard et al.*, 1998; *Lelieveld et al.*, 2001], is less seasonal. If we assume wetland and paddy emissions are near zero during the TRACE-P time period, annual inventories for anthropogenic CH_4 sources compiled for China and southeast Asian nations compiled by *Streets et al.* [2003] indicate that colocated urban/industrial sources (landfills, wastewater treatment, fossil fuel usage) would release roughly 38% of total emissions. Animal populations and coal mining, distributed more diffusely and in more rural regions, release on the order of 45%. Biomass and biofuel burning are estimated to contribute roughly 17%. The relative importance of various CH_4 sources varies widely between countries as well as between regions in large nations such as China, and therefore characteristic source trace gas signatures can vary widely for CH_4 depending upon individual air mass trajectories. For example, *Heald et al.* [2003] suggest that biomass burning in southeast Asia over the TRACE-P period of late spring was near its seasonal peak.

[6] In this report, we discuss a high-precision, high-resolution CH_4 data set sampled during the TRACE-P mission. The roughly 13,800 measurements were sampled at altitudes from roughly 12 km to the near-surface and range in magnitude from 1602 ppbv in stratospherically influenced air to 2149 ppbv in highly polluted air. Methane mixing ratios were highly correlated with those of a variety of other trace gases characteristic of a mix of industrial and combustion anthropogenic sources. Below we detail the CH_4 sampling methodology, followed by a description of the spatial distribution of CH_4 over the northern Pacific during TRACE-P. Section 4 compares the measurements to those made during the PEM West B mission, flown 7 years earlier under similar meteorological conditions.

2. Methodology

[7] Methane was measured on both the DC-8 and P-3B aircraft during TRACE-P, using the DACOM I and II instruments (Differential Absorption CO Measurement), respectively. These instruments are tunable diode laser systems [*Sachse et al.*, 1987, 1991] which simultaneously measure CH_4, CO, and N_2O. The same instrument system was used during PWB. DACOM uses three lasers (4.7, 4.5, and 7.6 microns for CO, N_2O, and CH_4 respectively) which are combined with optical filters and directed through a 0.3 l Herriott cell containing a 36 m long optical path. After exiting the cell, the laser beams are spectrally isolated and directed to separate LN_2-cooled InSb and HgCdTe detectors. A reference cell containing several Torr of each of the gases is used to wavelength lock each of the lasers to the

appropriate absorption lines. After being drawn through a permeable membrane dryer to remove water vapor, ambient air enters the Herriott cell, with a flow rate equivalent to twice the cell volume each second. The Herriott cell is maintained at 100 Torr to minimize potential spectral overlap from other atmospheric species. For typical ambient atmospheric levels, the differential absorption signals are proportional to the mixing ratios of the three measured gases [*Sachse et al.*, 1987]. Calibration of instrument response is performed by periodically flowing calibration gas with known near-ambient concentrations and zero air through the Herriot cell. Calibrations are performed approximately every 12 min with NOAA/CMDL calibration gases. Accuracies of the working standards are ±1% for CH_4 and ±2% CO (E. Dlugokencky and P. Novelli, personal communication, 2003). Consistency in the use of NOAA/CMDL standards on both the TRACE-P and PWB missions permits direct comparison of the samples collected on the missions, as well as with those collected as part of the CMDL clean air network. Although intercomparisons between measurements taken on the two aircraft include additional sources of error, *Eisele et al.* [2003] confirm excellent agreement during close proximity flight legs, with <0.1% deviation from a 1:1 regression slope.

[8] Although CH_4 measurements are made every 5 s, we have averaged the data to 60 s to integrate with other data sampled on the aircraft. Measurement precisions for CH_4 of ±0.15% (1 standard deviation) were obtained during TRACE-P. We estimate the overall accuracy of our measurements at ±1.02%, the majority of which is due to reference gas calibration. Methane data collected on the two aircraft are archived in their original resolution and can be obtained from the NASA-Langley Distributed Active Archive Center or through the GTE homepage (available at http://www-gte.larc.nasa.gov).

[9] Instrument problems during the early part of the mission, in particular the DC-8 transit flights from Dryden, California to Kona, Hawaii (flight 4) and Kona to Guam (flight 5), prevented the collection of DACOM CH_4 data on these flights. However, whole air samples were collected by the University of California at Irvine (UCI) for subsequent hydrocarbon and halocarbon analysis and these CH_4 data are available for some of this period. Details on sampling procedures used by the UCI group are given by *Blake et al.* [2003] and *Blake and Rowland* [1988]. Combining the UCI and DACOM CH_4 data sets however, requires a common calibration scale and establishing a relationship between the two data sets. Using the merged 60 s data, 462 "simultaneous" samples for which there are both UCI and DACOM measurements are available from DC-8 flights 7, 8, and 9. As would be expected, these data are highly correlated, with a small number of outliers likely due to differences in sampling intervals and/or high variability in the air being sampled (Figure 1a). The 23 measurements with differences greater than 2 standard deviations above the average difference were obtained during spirals when sequential samples indicate that variability was high. *Eisele et al.* [2003] further discuss some of the intercomparison complications created by differing integration times and constituent variability. Because UCI uses NIST CH_4 reference standards which differ from those of NOAA/CMDL used by DACOM, we expect a deviation from a 1:1 regression line between the

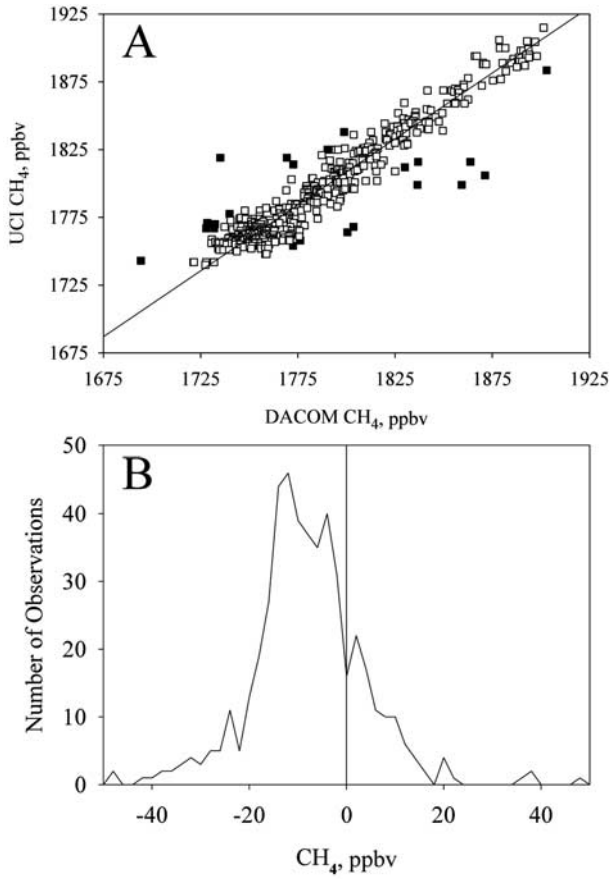

Figure 1. (a) Correlation between DACOM and UCI CH_4 measurements for "simultaneous" 1 min merged data. Solid squares denote data with differences >2 σ. (b) Frequency distribution of differences between DACOM and UCI CH_4 data. Differences average 9 ± 13 ppbv.

measurements. Differences between simultaneous samples averaged 9 ± 13 ppbv (UCI higher than DACOM) and were normally distributed, as would be expected for a calibration difference (Figure 1b). The average difference is consistent with the NIST/NOAA scale difference. Given the excellent correlation, the UCI data can be converted to DACOM values using the regression relationship and included for those periods during which the DACOM system was off-line. The UCI data make up 3% of the joint data set and have a standard error of 9 ppbv.

3. Methane Over the North Pacific Basin

[10] The regional distribution of CH_4 is illustrated in Figure 2, which shows 2.5° × 2.5° latitude/longitude averages for all of the data, divided into three altitude ranges, a lower, well-mixed boundary layer of 0–2 km, the midtroposphere of 2–6 km, and the upper troposphere, above 6 km. Because CH_4 sources are almost exclusively located on the continents and are greater in the Northern Hemisphere, mixing ratios would be expected to decrease with increasing altitude, with distance offshore, and with decreasing latitude. In addition to these general gradients seen in the TRACE-P data set, Figure 2 clearly demonstrates the elevated mixing ratios extending over a broad

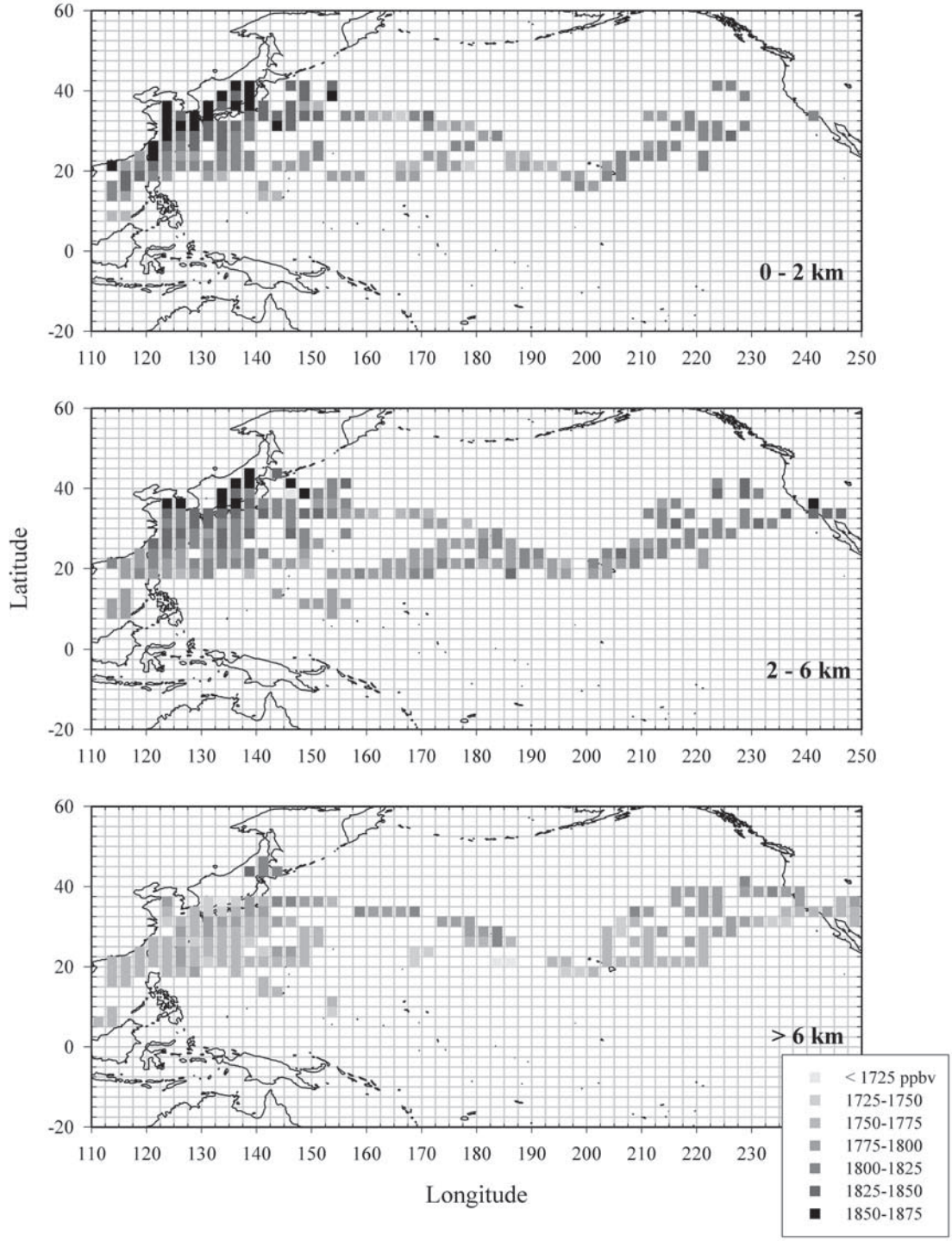

Figure 2. Regional distribution of CH_4 during the TRACE-P expedition; 0–2 km, 2–6 km, and above 6 km. Data were grouped into 2.5° latitude × 2.5° longitude areas then averaged. Number of observations within areas vary. See color version of this figure at back of this issue.

range of latitudes off the Asian continent as material is transported from Asia and further west into the basin. Concentrations decrease as long-lived trace gases such as CH_4 are transported from source regions and inputs are mixed vertically and horizontally at relatively rapid rates compared to photochemical loss. We can divide the area sampled during TRACE-P longitudinally to examine these gradients as continental outflow is advected across the North Pacific Basin by the dominant westerly flow [*Fuelberg et al.*, 2003]. Here, we break the region into two longitudinal classes, the Western Pacific, ranging from the coast of the Asian continent to 160°E, and the Central/Eastern Pacific, from 160°E to the North American coast. As Figure 2 illustrates, the sampling effort during TRACE-P

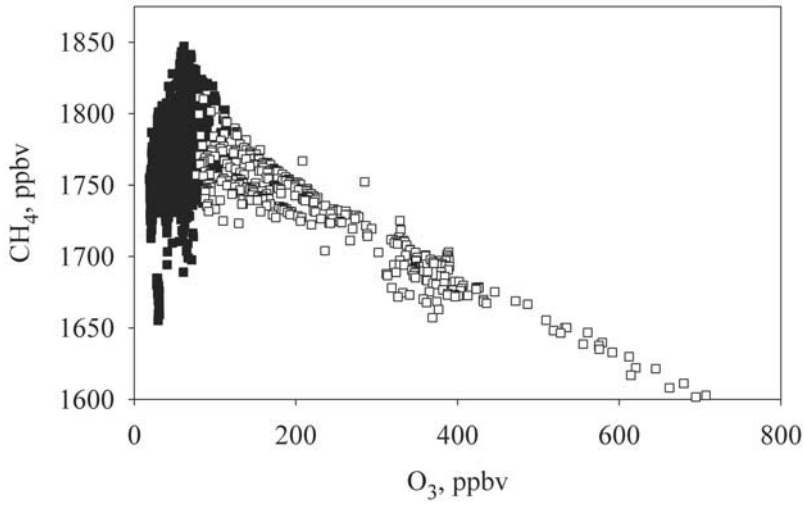

Figure 3. All TRACE-P data above 6 km. Open squares are observations classified as having a significant stratospheric input.

was concentrated largely within the Western Pacific class, and the majority of the data from the Central/Eastern Pacific class was obtained during transit flights.

[11] One of the primary concerns when characterizing the distribution of an environmental variable like CH_4 sampled over a large area such as the Pacific is evaluating how representative the intensive, but relatively brief sampling is of the regional distribution. This evaluation is particularly critical if the derived distributions are to be compared to other times or areas. As detailed by *Jacob et al.* [2003], flights conducted during TRACE-P and other similar aircraft missions were designed to meet a variety of objectives, only one of which is a regional characterization. One way to approach this problem is to compare the sampled three-dimensional distributions with those derived from models, integrated on a variety of temporal and spatial scales [*Kiley et al.*, 2003; *Wild et al.*, 2003]. The representativeness of sampled distributions based on the much sparser PWA and PWB data sets has been examined in some detail by *Ehhalt et al.* [1997], who concluded that the ethane and propane distributions were reasonable descriptions of the ''true'' average pattern of concentrations, despite incomplete and irregular sampling. Although this work dealt with shorter-lived hydrocarbons and clearly every aircraft mission differs, the use of two aircraft and the much more geographically extensive sampling performed during TRACE-P suggest that the derived distributions, as shown in Figure 2, are an adequate representation of true geographic patterns over the sampling period.

[12] Averages shown in Figure 2 include the entire data set and therefore include observations which were affected by inputs from the stratosphere. Although most frequently seen at altitudes above 6 km and latitudes above 35°N [*Browell et al.*, 2003], stratospherically impacted air was observed at a variety of locations throughout the mission and serves as a mechanism introducing very low CH_4 mixing ratios to the troposphere. These significantly lower mixing ratios, however, can mask the variability due to mixing and transport that is the focus of TRACE-P. For this reason, we have elected to remove observations identified as having significant stratospheric inputs from subsequent analysis. As shown in Figure 3, air with a significant stratospheric component has a distinctive signature, with elevated O_3 and low CH_4 (as well as CO, C_2H_6, C_2H_2, and other trace gases, data not shown). Here, we removed from further analysis all observations with low CH_4 and O_3 levels greater than about 100 ppbv, or with CH_4/O_3 ratios less than about 20, a total of about 450 observations (3% of the data). At altitudes below 6 km, air classified as having a significant stratospheric component was <1% of the data. These observations appear to fall on a mixing line between clearly stratospheric air and observations more characteristic of Northern Hemisphere levels. They form a well defined group that overlaps but is distinct from the distribution of mixing ratios at upper altitudes (Figure 4).

3.1. Variability With Latitude

[13] Methane exhibits a well-known, seasonally varying latitudinal trend in background surface-level mixing ratios, from high values in the Northern Hemisphere to lower levels in the Southern Hemisphere [*Dlugokencky et al.*, 1994]. Monthly averages of background air measurements at Pacific basin Climate Monitoring and Diagnostic Laboratory (CMDL) ground-level sites provide a way to estimate the enhancements due to Asian outflow observed during TRACE-P. We have derived background CH_4 levels by weighting the Pacific CMDL February, March, and April 2001 monthly means for the TRACE-P sampling period and then grouping and averaging every 5° of latitude to reduce site-specific variability.

[14] As shown in Figure 5a, Western Pacific average CH_4 mixing ratios in the lower 2 km are elevated well above Pacific CMDL background levels north of 15°N. These enhancements range between 27 and 38 ppbv and background levels lie well outside the 95% confidence limits for the TRACE-P means. The largest differences between CMDL levels and those sampled in the Western Pacific are between 15° and 20°N and 30° and 35°N, probably reflecting outflow from Hong Kong and Japan. Averages to the south, between the equator and 15°N, were comparable to CMDL site values. These background levels lie within the TRACE-P 95% confidence limits. At higher altitudes, mixing ratios are significantly lower than surface back-

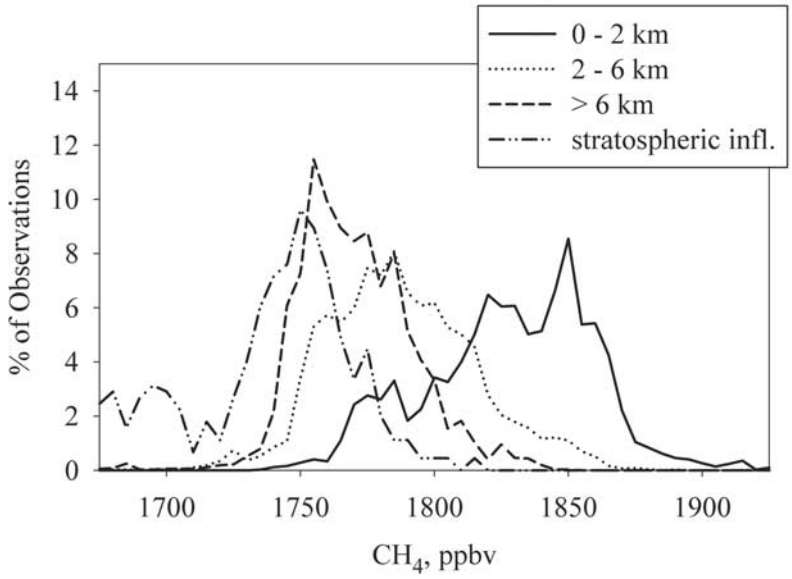

Figure 4. Frequency distribution for all TRACE-P data by altitude.

ground values and decrease with increasing altitude by a variable amount. Note that low, relatively constant concentrations extend from 25° to 5°N above 6 km, from roughly 15° to 5°N at 2–6 km, and are absent in the near-surface; differences reflecting the mixing of Northern and Southern Hemispheric air at upper altitudes and the northward penetration of Southern Hemispheric air with characteristically lower mixing ratios of many trace gases. The air south of 25°N and at altitudes >6 km averaged CO levels between 75 and 100 ppbv, mean C_2Cl_4 mixing ratios of ~2.4 pptv, and C_2H_2/CO ratios of 0.9–1.3. Latitudinal distributions for a variety of other trace gases including C_2H_6, C_2H_2, C_3H_8, and C_2Cl_4 had similar latitudinal gradients and relative differences with altitude as those for CH_4.

[15] At Central/Eastern Pacific longitudes (Figure 5b), near-surface average CH_4 mixing ratios are much lower and more similar to CMDL background values as would be expected as distance from sources increases. Aside from the 30–35°N latitude band, however, the CMDL values are outside the 95% confidence intervals. Central/Eastern latitude means are between 8 and 40 ppbv lower than Western Pacific averages, with greatest differences to the north. Average mixing ratios above 6 km, however, are significantly greater than those at 2–6 km between 30 and 35°N and are indistinguishable from other averages at latitudes north of 25°N. Between 25 and 35°N, these high altitude means are significantly higher than averages at these latitudes in the Western Pacific (10 ppbv between 30 and 35°N; 7 ppbv, 25–30°N). These higher concentrations of CH_4 are seen in the bottom panel of Figure 2 between 160° and roughly 180°E and are associated with enhanced CO, C_2H_6, CH_3Cl, and C_2Cl_4, among other gases. Coinciding with the most intense position of the Japan Jet [*Fuelberg et al.*, 2003], these continental emissions appear to be rapidly and efficiently carried at higher altitudes to the Central Pacific.

3.2. Variability With Longitude

[16] Because CH_4 sources and therefore atmospheric mixing ratios, change systematically with latitude [*Dlugokencky*

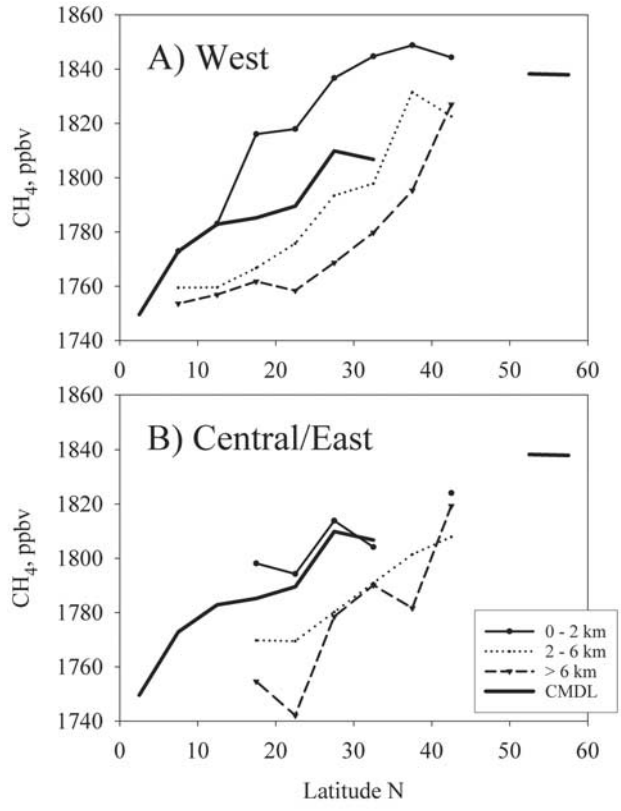

Figure 5. (a) Latitudinally averaged CH_4 mixing ratios in the Western Pacific (west of 160°E), 5° latitude classes. Averaged CMDL values are for Pacific Basin sites only and are calculated by weighting monthly averages for the TRACE-P sampling period and then averaging into 5° latitude classes. CMDL sites included were American Samoa; Cape Grim, Australia; Cold Bay and Shemya Island, AK; Christmas Island; Easter Island; Guam; Mauna Loa and Cape Kumukahi, HI; and Pacific Ocean cruise stations. (b) As for Figure 5a, Central/Eastern Pacific (east of 160°E).

et al., 1994], any examination of longitudinal trends must account for this known source of variability. We have therefore grouped the TRACE-P observations into latitude classes, which largely correspond to the trajectory-based source region classes developed during the PWB mission, Continental North (>20°N) and Continental South (<20°N) [*Talbot et al.*, 1997]. The three TRACE-P latitude classes, South (<20°N, actually 7°N–20°N), Middle (20°N– 40°N), and North (>40°N, actually 40°N–46°N), subdivide the PWB Continental North group to permit examination of the most intensely sampled TRACE-P region. As shown in Figure 6a, data from the North latitude class are spatially sparse and suggest only that mixing ratios fall offshore. At latitudes south of 20°N (Figure 6c), concentrations close to the Asian continent are elevated in the near-surface only and decrease to CMDL background levels beyond 140°E. Five-day back trajectories for the data used in these averages indicate that those in the near-surface between 110° and 140°E are predominantly from the north and west over central Asia, and China, while those above 2 km are dominated by oceanic pathways, more southerly flows from southeast Asia, or westerly flow extending back to India or Africa. These general trends are in agreement with those reported by *Bey et al.* [2001], based on modeling PWB data.

[17] Between 20° and 40°N, elevated CH_4 is most clearly seen below 6 km and extends to roughly 160°E before sharply falling (Figure 6b). Higher concentrations are also seen off the North American coast at all altitudes. Five-day back trajectories indicate that much of the air sampled over the east Pacific had been transported east across Asia into the Pacific basin, then circulated around a strong high pressure system centered in this region [*Fuelberg et al.*, 2003]. Air masses from the high northern latitudes were also transported to eastern Pacific midlatitudes by the high.

[18] Although differences in sampling effort with latitude within the longitude band may contribute to apparent longitudinal trends, Figure 6b and CMDL background levels in Figure 5 suggest that an average mid-Pacific mixing ratio in the near-surface between 20° and 40°N is on the order of 1785 ppbv. Near-surface levels off the Asian continent (below 2 km and west of 160°E) are roughly 45 ppbv higher. At altitudes between 2 and 6 km, averages have been increased on the order of 15 ppbv. Restricting the calculation of longitudinal averages to a 10° latitude band of 15–25°N (data not shown) where sampling is more consistent latitudinally (Figure 2), yields an average enhancement of 36 ppbv at altitudes below 2 km west of 160°E. Little change with longitude is seen above 2 km, suggesting that much of the transport of continental inputs occurred in the near-surface and that apparent enhancements at these altitudes in the broader longitude class are primarily due to differential sampling with latitude.

[19] Strong longitudinal trends are also seen in averages for other trace gases, a subset of which is shown in Figure 7. Trends in CH_4 are particularly well correlated with those of other hydrocarbons such as ethane (C_2H_6; Figure 7b), ethyne (C_2H_2; Figure 7c), and propane (C_3H_8; data not shown). Longitudinal variation in CO (Figure 7a) is similar to CH_4 but shows only modest elevation off the coast of North America. Note that the trends in C_2H_2 are more similar to those for CO as would be expected, since

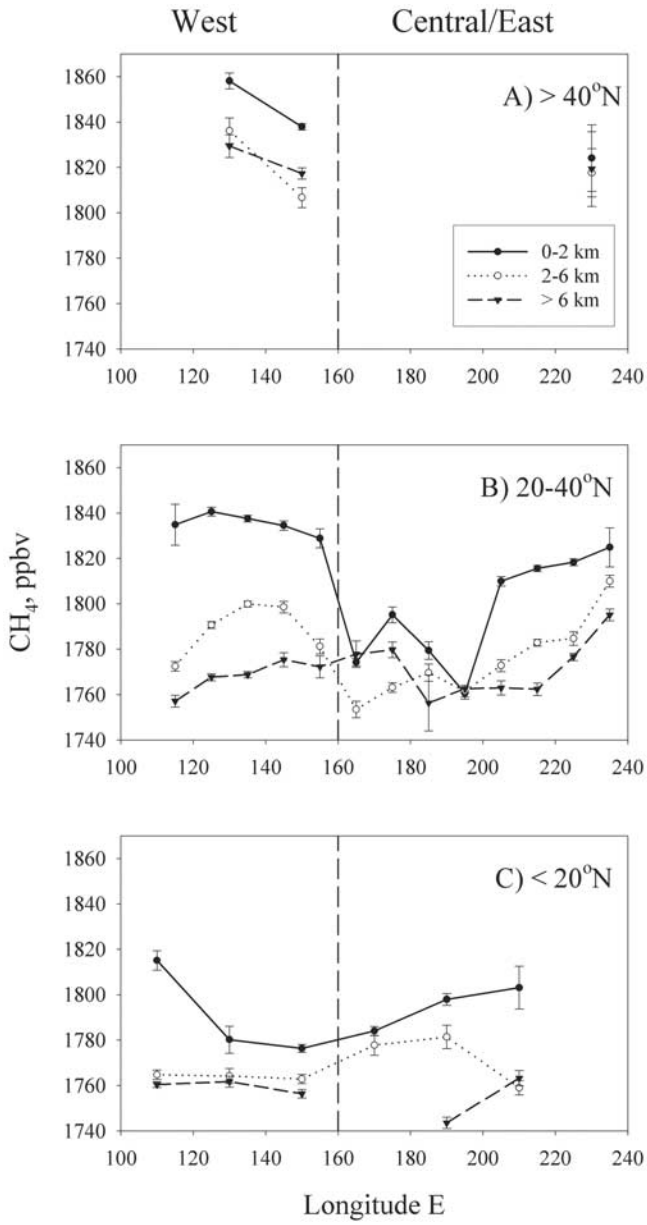

Figure 6. Longitudinally averaged CH_4 mixing ratios by latitude class. Error bars indicate 95% confidence intervals. Dashed line at 160°E marks the break between the Western Pacific longitude class and the Central/Eastern Pacific class. Note that west longitudes (east of 180°E) are scaled as a continuation of east longitudes. (a) North of 40°N; (b) 20°N–40°N; (c) South of 20°N.

emission ratios for these gases from all types of combustion are very similar [*Blake et al.*, 1996].

[20] Also shown in Figures 6 and 7 are the enhanced levels of CH_4 and other gases above 6 km in the central Pacific from roughly 160°W–170°E, discussed in Section 4.1. Concentration ratios of simultaneously measured trace gas species such as the nonmethane hydrocarbons (NMHCs) can provide a rough estimate of air mass aging and mixing if they are released concurrently, if they are photochemically removed by reactions that approximate first order kinetics, if background concentrations into which they are mixed are

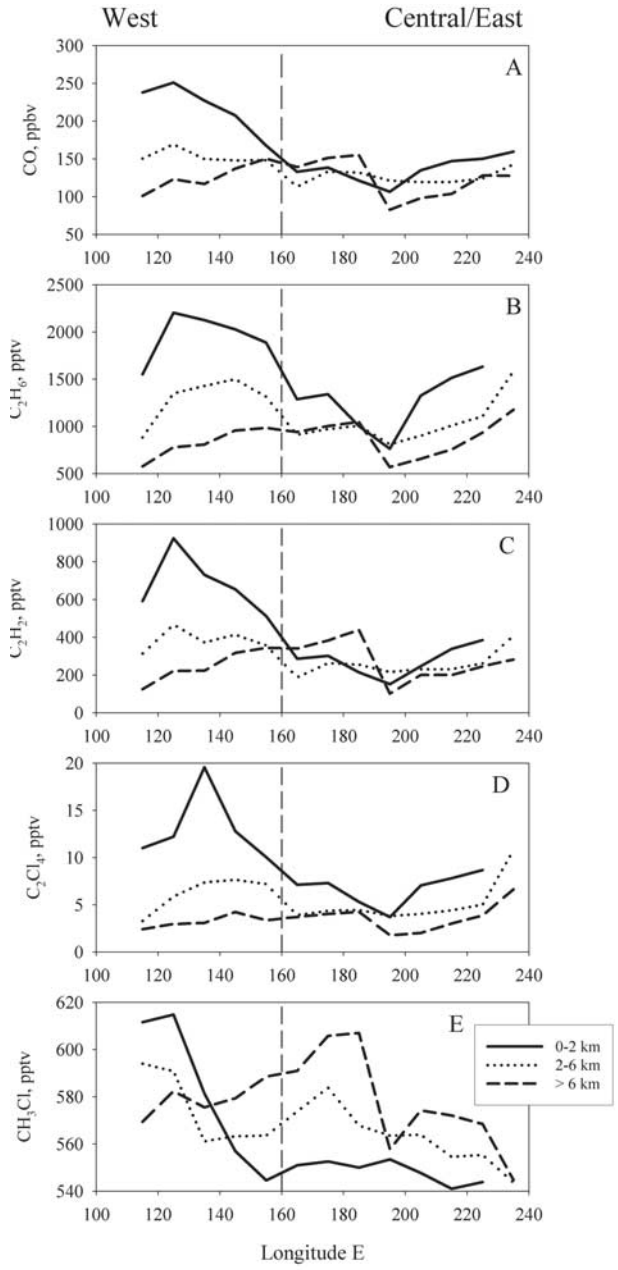

Figure 7. As for Figure 6b, averages with longitude within 20°N–40°N. Note that west longitudes (east of 180°E) are scaled as a continuation of east longitudes. (a) CO; (b) C_2H_6; (c) C_2H_2; (d) C_2Cl_4; and (e) CH_3Cl.

negligible, and if removal rates are significantly different [*McKeen et al.*, 1996; *Parrish et al.*, 1992]. Ratios of C_2H_2/CO and C_3H_8/C_2H_6 have been used in this way by a variety of investigators [*Talbot et al.*, 1997; *Gregory et al.*, 1997; *Smyth et al.*, 1996]. Both ratios are elevated in this region over those further to the east, and averages range from 2.3 to 2.5 and from 0.12 to 0.13, respectively. These values suggest that only several days have elapsed since emission. The use of tracers such as C_2Cl_4, indicative of urban and industrial sources [*Blake et al.*, 1997; *Wang et al.*, 1995], and CH_3Cl, produced predominantly during biomass burning [*Rasmussen et al.*, 1980; *Blake et al.*, 1996] can help clarify origins of these increased levels at high altitude. Enhancements in both compounds (Figures 7d and 7e) indicate that elevated levels of trace gases at Western Pacific longitudes have a variety of sources, as might be expected. At high altitudes over the central Pacific however, C_2Cl_4 is not particularly high and CH_3Cl is strongly enhanced, suggesting that emissions from biomass burning or the burning of biofuels may be the primary source. Methane and CO are highly correlated in this air mass ($r^2 = 0.77$; n = 177) and yield a regression slope ($\Delta CH_4/\Delta CO$) of 0.39, consistent with biomass burning emission ratios [*Andreae and Merlet*, 2001]. Mixing ratios of CH_4, CO, C_2H_6, and C_2H_2 are also highly correlated with CH_3Cl, with regression slopes within combustion emission ranges ($\Delta CH_4/\Delta CH_3Cl$ = 0.58 ppbv/pptv, $r^2 = 0.45$; $\Delta CO/\Delta CH_3Cl$ = 1.76 ppbv/pptv, $r^2 = 0.85$; $\Delta C_2H_6/\Delta CH_3Cl$ = 10.4, $r^2 = 0.76$; $\Delta C_2H_2/\Delta CH_3Cl$ = 7.1, $r^2 = 0.82$; n = 94). Five-day back trajectories show that most of this air passed across southeast Asia, southern China, and northern India where biomass and biofuel burning occurs at this time of year [*Heald et al.*, 2003; *Lelieveld et al.*, 2001]. *Andreae and Merlet* [2001] suggest that the common Indian practice of burning dung cakes for fuel results in enhanced CH_3Cl release in particular from this region. Additional characteristics of this plume are discussed by *Blake et al.* [2003] and C.L. Heald et al. (Transpacific satellite and aircraft observations of Asian pollution, submitted to *Journal of Geophysical Research*, 2003).

[21] A regional characterization of the North Pacific Basin during TRACE-P for selected trace gases is summarized in Table 1 for the three altitude classes (0–2 km, 2–6 km, and >6 km), the three latitudinal classes (<20°N, 20°–40°N, and >40°N), and the two longitudinal classes (110°–160°E and 160°–240°E).

3.3. Variability With Altitude

[22] In the preceding sections we have used broad altitude classes to group and discuss two-dimensional spatial trends. In this section we examine trends with altitude more closely within the more intensely sampled West Pacific and contrast them with those from the Central/East Pacific. As shown in Figure 8a, average CH_4 mixing ratios at latitudes south of 20°N are relatively constant above roughly 4 km and are not significantly different. Concentrations increase sharply below, reflecting surface inputs. Profile shapes are similar for C_2H_6 (Figure 8b) and CO (Figure 8e). Between the latitudes of 20°N and 40°N, averaged CH_4 levels are higher and increase smoothly throughout the air column. Mixing ratios below 9 km are significantly higher than those south of 20°N. Aside from concentrations in the lowest km, averages for latitudes above 40°N are significantly higher than those at lower latitudes. In the Central/Eastern Pacific (Figure 8f), concentrations are significantly lower than those in the West. Exceptions to this generalization are averages for 3–4 km (below 20°N and north of 40°N) and between 6 and 10 km (20°N–40°N), discussed in the preceding section.

[23] In both the Western and Central/Eastern Pacific, variability in CH_4 concentrations with altitude are strikingly correlated with a number of other trace gases, most notably those of C_2H_6 (Figures 8b and 8g) and C_2Cl_4, which has sources that are specific to urban/industrial activities such as dry cleaning and industrial degreasing (Figures 8c and 8h). Although correlations are slightly higher over the Western

Table 1. TRACE-P Regional Characterization for Selected Trace Gases[a]

Longitude	Latitude	Altitude, km	CO, ppbv	CH_4, ppbv	CO_2, ppmv	C_2Cl_4, pptv	CH_3Cl, pptv	C_2H_6, pptv	C_2H_2, pptv	C_3H_8, pptv	C_2H_2/CO, pptv/ppbv
West (west of 160°E)	<20°N	0–2	187 ± 6	1803 ± 2	374 ± 0.1	7.0 ± 0.2	608 ± 5	1385 ± 46	579 ± 36	290 ± 17	2.4 ± 0.06
		2–6	102 ± 1	1764 ± 1	372 ± 0.1	3.1 ± 0.1	565 ± 1	685 ± 14	155 ± 8	63 ± 4	1.3 ± 0.03
		>6	96 ± 1	1760 ± 1	371 ± 0.1	2.4 ± 0.04	578 ± 2	610 ± 10	122 ± 4	60 ± 3	1.2 ± 0.02
	20°–40°N	0–2	232 ± 2	1838 ± 1	377 ± 0.1	14.5 ± 0.5	592 ± 2	2111 ± 16	790 ± 15	716 ± 12	3.2 ± 0.02
		2–6	156 ± 1	1793 ± 0.4	374 ± 0.03	6.5 ± 0.1	576 ± 1	1362 ± 12	410 ± 6	294 ± 5	2.3 ± 0.02
		>6	120 ± 1	1769 ± 1	372 ± 0.03	3.1 ± 0.1	578 ± 1	798 ± 11	227 ± 6	109 ± 4	1.7 ± 0.02
	>40°N	0–2	202 ± 7	1844 ± 2	378 ± 0.2	11.3 ± 0.4	546 ± 4	2249 ± 41	700 ± 35	779 ± 26	3.5 ± 0.04
		2–6	169 ± 5	1817 ± 2	376 ± 0.2	9.9 ± 0.3	551 ± 2	1815 ± 50	520 ± 25	516 ± 24	3.0 ± 0.06
		>6	163 ± 2	1822 ± 2	376 ± 0.1	10.9 ± 0.3	541 ± 1	1899 ± 48	500 ± 21	567 ± 28	3.0 ± 0.06
Central/East (east of 160°E)	<20°N	0–2	123 ± 1	1798 ± 3	374 ± 0.1	5.8 ± 0.1	543 ± 2	1070 ± 17	187 ± 4	115 ± 4	1.5 ± 0.02
		2–6	135 ± 4	1775 ± 2	373 ± 0.1	3.9 ± 0.2	578 ± 5	897 ± 34	277 ± 22	90 ± 8	1.9 ± 0.09
		>6	76 ± 1	1751 ± 3	371 ± 0.3	0.8 ± 0.3	546 ± 2	496 ± 40	71 ± 15	21 ± 5	0.9 ± 0.1
	20°–40°N	0–2	137 ± 1	1798 ± 1	374 ± 0.1	7.2 ± 0.1	547 ± 1	1362 ± 20	304 ± 6	274 ± 8	2.1 ± 0.03
		2–6	126 ± 1	1773 ± 1	373 ± 0.03	4.6 ± 0.1	565 ± 1	1008 ± 11	248 ± 5	141 ± 4	1.8 ± 0.02
		>6	124 ± 1	1776 ± 1	373 ± 0.04	3.7 ± 0.1	574 ± 1	892 ± 14	260 ± 8	109 ± 4	1.8 ± 0.03
	> 40°N	0–2	134 ± 1	1824 ± 2	374 ± 0.1	7.7 ± 0.2	534 ± 1	1489 ± 26	380 ± 8	453 ± 15	2.8 ± 0.05
		2–6	137 ± 9	1818 ± 3	374 ± 0.3	7.0 ± 0.5	556 ± 6	1428 ± 77	412 ± 56	376 ± 30	2.6 ± 0.1
		>6	178 ± 4	1819 ± 3	374 ± 0.1	6.6 ± 0.3	612 ± 8	1426 ± 49	609 ± 54	311 ± 13	3.1 ± 0.07

[a]Average values and standard error of the means for broad longitude, latitude, and altitude classes.

Pacific, the coefficient of determination (r^2) between these spatially averaged CH_4 and C_2H_6 mixing ratios is 0.97 and for CH_4 and C_2Cl_4 is 0.92 (n = 63). The slope of the regression line with C_2H_6 ($\Delta CH_4/\Delta C_2H_6$) is 0.05 ppbv/pptv and with C_2Cl_4 is 7.37 ppbv/pptv. Although the relationship with CO is not as tight (r^2 = 0.81; n = 65), correlation between the two is still excellent overall, with a CH_4:CO regression slope of 0.58, suggesting a mixture of urban ($\Delta CH_4/\Delta CO \sim 1$) [*Harriss et al.*, 1994; *Harris et al.*, 2000; *Bartlett et al.*, 1996] and combustion sources ($\Delta CH_4/\Delta CO$ 0.03 − 0.1) [*Scholes et al.*, 1996; *Bartlett et al.*, 1996; *Ferek et al.*, 1998; *Andreae and Merlet*, 2001]. Major sources of C_2H_6, largely dominated by emissions from the Northern Hemisphere, are believed to be natural gas losses and biomass burning [*Rudolph*, 1995]. The tight correlation between C_2H_6 and CH_4 (Figure 9) would suggest that these sources also predominate for CH_4 during TRACE-P or that the colocated mix of urban/industrial sources of the two gases is relatively constant. Enhancements of CH_4 from sources such as rice paddies and ruminant enteric fermentation that are not sources of C_2H_6 [*Streets et al.*, 2003] were not observed and appear not to have made major contributions to the sampled air masses.

[24] We can further breakdown the Western Pacific longitude class to examine trends in more detail close to the Asian continent. As demonstrated in Figure 10 for 20° longitude means, there is clear coherence between average altitude profiles of all the hydrocarbons shown. Elevated CH_4 is generally confined to altitudes <4 km west of 120°E. As air is carried away from the Asian continent, near-surface levels tend to decrease and those at high altitudes tend to increase as mixing takes place vertically and horizontally. Regression slopes between CH_4 and C_2H_6 ($\Delta CH_4/\Delta C_2H_6$) vary from 0.076 ($r^2$ = 0.98) in the lower 4 km west of 120°E, to 0.050–0.052 ppbv/pptv (120°–140°E and 140°–160°E) for these means. Although high throughout the region, the slope of propane to ethane ($\Delta C_3H_8/\Delta C_2H_6$) decreases in a consistent west-to-east pattern; 0.51 (<4 km, west of 120°E), 0.44 (120°1–140°E), 0.44 (140°–160°E), and 0.35 (160°–180°E) as air masses begin to age and the shorter lived propane is photochemically oxidized more rapidly than ethane and mixed to lower background levels. Variability in CH_4, C_2H_6, C_2H_2, and C_3H_8 is poorly correlated with CH_3Cl and emission ratios between CH_4 and these NMHCs lie outside the range reported for biomass burning [*Andreae and Merlet*, 2001].

3.4. Transport Pathways and Plumes

[25] Because the majority of the TRACE-P sampling was conducted north of 20°N, we expect that Northern Hemisphere anthropogenic sources should dominate emissions of many gases. The high correlation between CH_4 and the urban/industrial tracer C_2Cl_4, as well as the striking correspondence between hydrocarbon species with predominantly anthropogenic sources suggests that the continental outflow to the region sampled by TRACE-P has a predominantly anthropogenic signature during the late February-early April period. There were however, air masses sampled that had a variety of trace gas signatures since source spatial heterogeneity is high and transport from regions as distant as Europe and Africa can be seasonally significant [*Bey et al.*, 2001; *Liu et al.*, 2003]. Because of the relatively long atmospheric lifetime of CH_4, air masses can retain distant source signatures until mixed and modified. *Bey et al.* [2001] characterize spring continental outflow to the Pacific as following three main pathways: lifting by southeastward-moving cold fronts, followed by eastward transport in the lower free troposphere; boundary layer transport behind cold fronts; and convective transport, primarily over southeast Asia at this time of year. In this section we examine examples of elevated trace gases to investigate source variability in somewhat more detail and to characterize CH_4 transport via the primary outflow mechanisms. Use of tracers such as C_2Cl_4 for industrial activities, CH_3Cl and C_2H_2 for combustion, and C_2H_2/CO ratios as a general indicator for air mass age aide in source-type and region identification. Correlations between selected species for plumes grouped by primary transport path are summarized in Table 2.

[26] Some of the highest CH_4 mixing ratios sampled during TRACE-P were seen during occasions when the

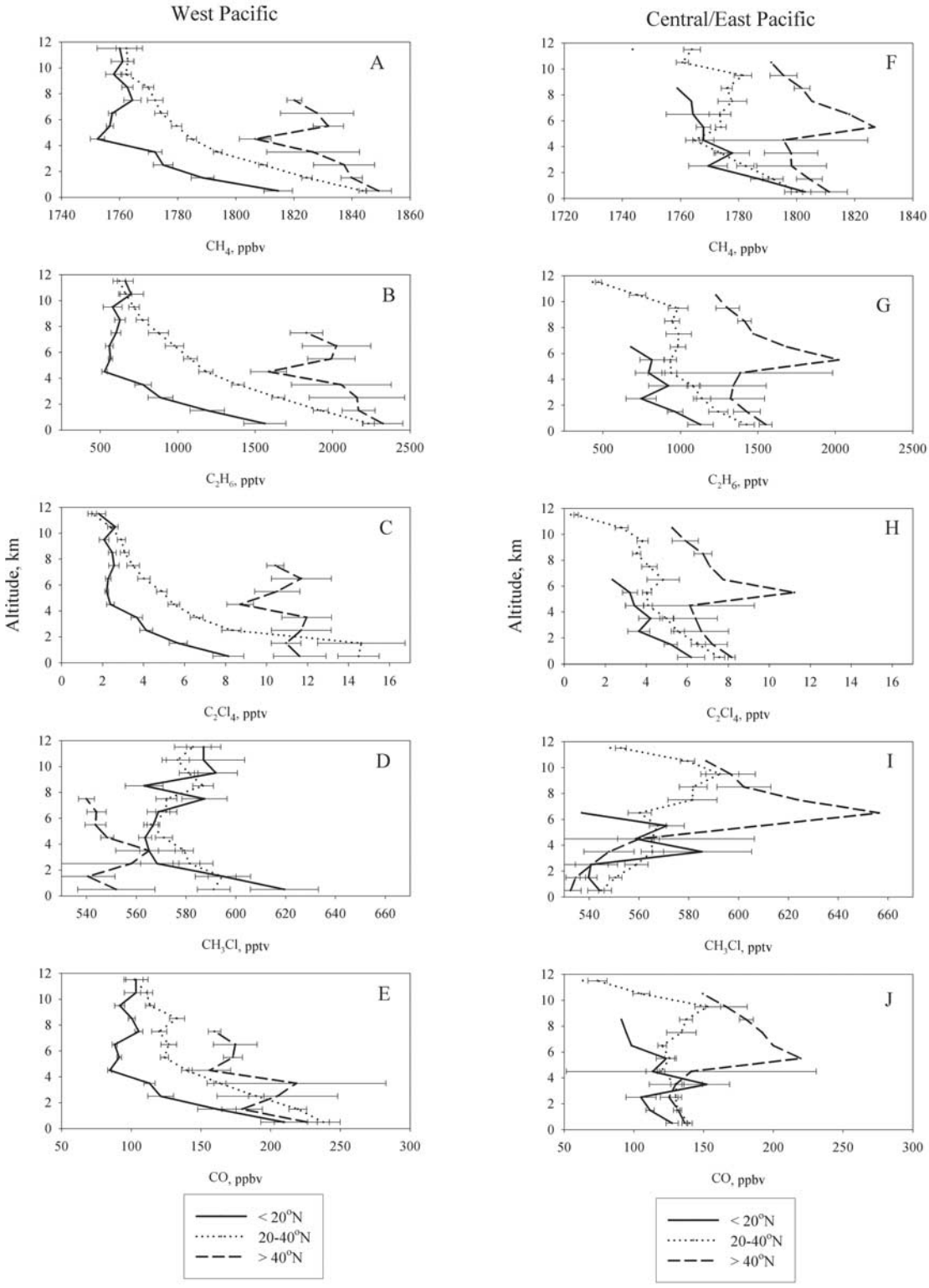

Figure 8. Average altitude profiles by latitude class. Error bars denote 95% confidence intervals. For the Western Pacific (west of 160°E): (a) CH_4; (b) C_2H_6; (c) C_2Cl_4; (d) CH_3Cl; (e) CO. For the Central/Eastern Pacific (east of 160°E): (f) CH_4; (g) C_2H_6; (h) C_2Cl_4; (i) CH_3Cl; (j) CO.

aircraft intercepted highly polluted air in boundary layer outflow behind cold fronts. This occurred during DC-8 flight 13 in the Shanghai area on 21 March over a period of roughly 50 min (Figure 11). Methane levels ranged up to 1983 ppbv within this air mass and averaged 1866 ppbv. Finer resolution data using the original 5 s sampling interval captured higher and more variable mixing ratios. Enhanced levels were correlated with a variety of other species including CO, as shown in Table 2, suggesting a complex mixture of co-located combustion, industrial, and

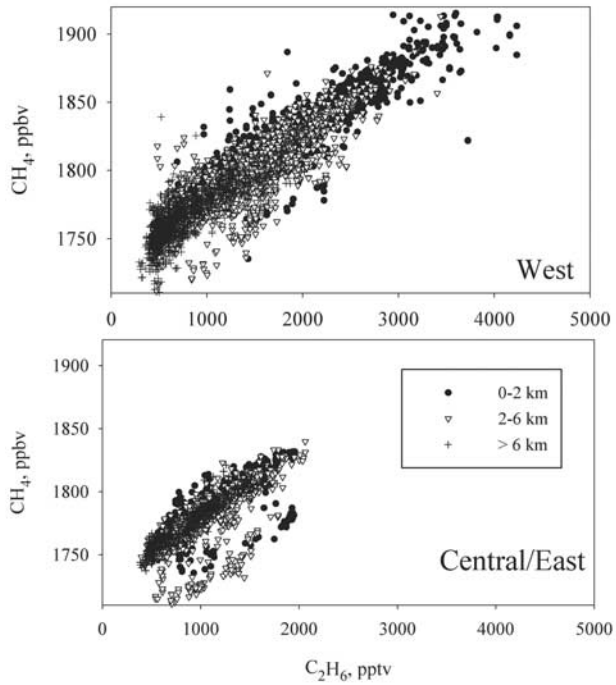

Figure 9. Correlation between CH_4 and C_2H_6, 60 s averages, all TRACE-P data. (a) Western Pacific (west of 160°E), n = 5800; and (b) Central/Eastern Pacific (east of 160°E), n = 2050.

fossil fuel sources. Because levels of CH_3Cl were extremely high (up to 1677 pptv) and the $\Delta CH_4/\Delta CO$ was relatively low (0.22), combustion inputs appear to have been sizable. Carbon monoxide was also well correlated with CH_3Cl and regression yields a relatively high emission ratio ($\Delta CH_3Cl/\Delta CO$ = 1.24 pptv/ppbv; r^2 = 0.85) but one consistent with those reported by *Lobert et al.* [1991], *Blake et al.* [1996], and *Andreae et al.* [1996], particularly for smoldering combustion. Since the source area of Shanghai is highly urban, biofuel combustion (in cookstoves or for domestic heating, for example) or perhaps low-quality coal use rather than biomass burning are the more likely combustion sources. Other instances of polluted Asian boundary layer outflow were sampled on DC-8 flight 12 and P-3B flight 19, with similar characteristics (Table 2).

[27] The major process transporting polluted Asian air masses during TRACE-P is the passage of southeastward-moving cold fronts across the continent, followed by eastward transport in the lower free troposphere [*Liu et al.*, 2003]. Frontal passage is at a seasonal high in the spring and fall and occurs roughly every 2–7 days. A number of polluted air masses intercepted during TRACE-P had 5-day trajectories extending back to the northwest that fall into this class (Table 2). These plumes were generally below 6 km altitude, had relatively low inputs from biomass burning, as indicated by low CH_3Cl mixing ratios and poor or negative correlations between CH_3Cl and other trace gases, and were enriched in C_2Cl_4, a northern hemisphere industrial tracer. Although $\Delta CH_4/\Delta CO$ values vary, they average a relatively high 0.55 ± 0.24 (Table 2) , also suggesting that recent combustion inputs were low.

[28] Deep convection over Southeast Asia followed by northeast transport and frontal lifting moves biomass burning emissions into the Asian midlatitudes where they are mixed with those from farther north. A variety of plumes sampled off the Asian continent had back-trajectories that extended to the west and southwest across southern China, northern southeast Asia and extending back to India and

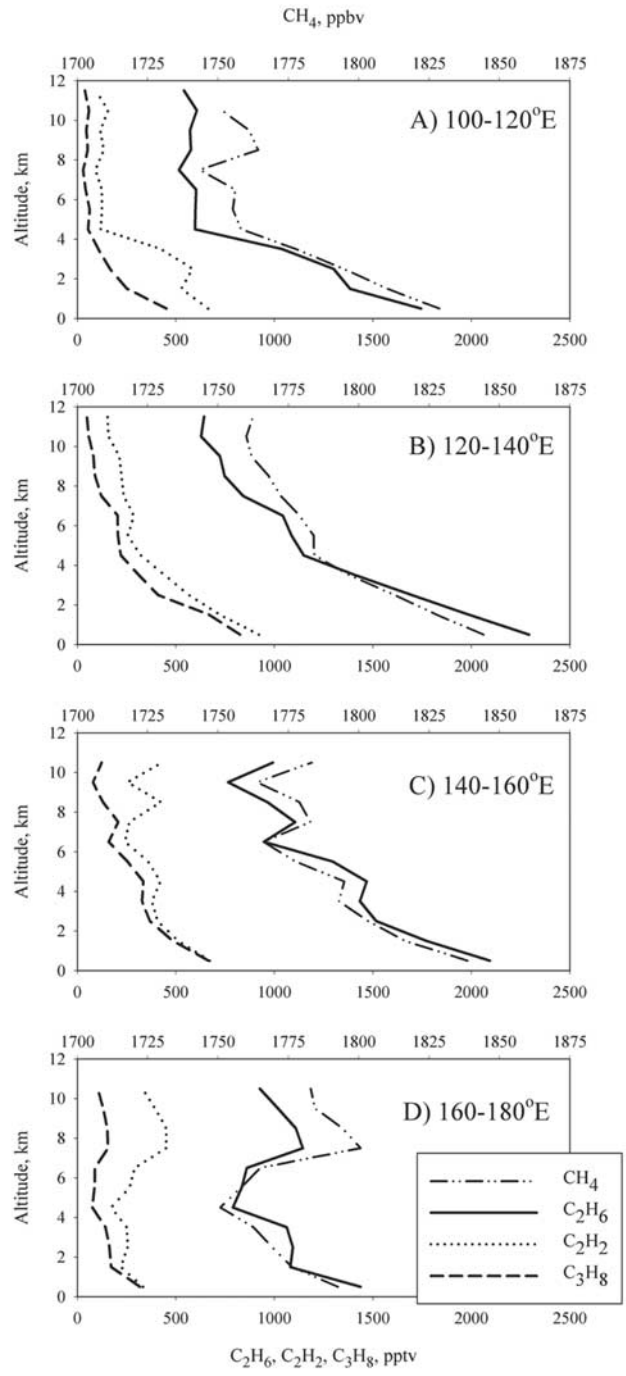

Figure 10. Average altitude profiles for CH_4 and selected hydrocarbons, 20°N–40°N; 20° longitude classes. (a) 100–120°E; (b) 120–140°E; (c) 140–160°E; and (d) 160–180°E.

Table 2. Correlations Between Selected Trace Gases in Case Studies or Plumes[a]

Flight	Air Mass	CH_4:CO, ppbv:ppbv	CH_4:CO_2, ppbv:ppmv	CH_4:C_2H_6, ppbv:pptv	CH_4:C_2H_2, ppbv:pptv	CH_4:C_3H_8, ppbv:pptv	CH_4:C_2Cl_4, ppbv:pptv	CH_4:CH_3Cl, ppbv:pptv	CO:CO_2, ppbv:ppmv	C_2H_6:CO pptv:ppbv
					Boundary Layer Outflow					
DC-8, 13	Shanghai; N = 47, N_{HC} = 37	0.22 (0.90)	8.84 (0.57)	0.052 (0.84)	0.021 (0.81)	0.052 (0.73)	1.65 (0.73)	0.16 (0.81)	42.7 (0.71)	3.55 (0.76)
DC-8, 12	Formosa Strait; N = 50, N_{HC} = 30	0.31 (0.93)	8.64 (0.91)	0.048 (0.97)	0.047 (0.94)	0.069 (0.93)	4.87 (0.95)	0.18 (0.78)	27.8 (0.96)	6.39 (0.93)
P-3B, 19	near-surface; N = 195, N_{HC} = 91	0.27 (0.84)	6.37 (0.60)	0.044 (0.83)	0.064 (0.79)	0.052 (0.71)	1.66 (0.39)	0.66 (0.73)	20.4 (0.52)	6.16 (0.87)
	Average	0.27	7.95	0.048	0.044	0.058	2.72	0.33	30.3	5.37
	Standard Deviation	0.045	1.37	0.004	0.022	0.01	1.86	0.28	11.4	1.58
					NW Trajectories					
DC-8, 19	near-surface plume; N = 248, N_{HC} = 142	0.62 (0.70)	16.5 (0.82)	0.050 (0.70)	0.148 (0.58)	0.126 (0.52)	8.01 (0.80)	NS	20.5 (0.71)	9.53 (0.61)
DC-8, 19	above ~5 km; N = 306, N_{HC} = 159	0.33 (0.73)	12.2 (0.83)	0.048 (0.79)	0.106 (0.62)	0.292 (0.71)	10.6 (0.71)	NS	32.3 (0.91)	7.23 (0.90)
DC-8, 18	below 6 km; N = 279, N_{HC} = 155	0.81 (0.88)	15.5 (0.90)	0.054 (0.92)	0.17 (0.88)	0.14 (0.88)	9.39 (0.91)	NS	17.8 (0.91)	14.8 (0.88)
DC-8, 10	near-surface; N = 148, N_{HC} = 62	0.39 (0.75)	13.6 (0.86)	0.051 (0.76)	0.123 (0.88)	0.087 (0.34)	7.68 (0.81)	1.20 (0.43)	28.5 (0.91)	7.48 (0.55)
DC-8, 14	Low altitude plume; N = 203, N_{HC} = 108	0.71 (0.72)	12.4 (0.72)	0.051 (0.82)	0.132 (0.68)	0.104 (0.75)	6.98 (0.75)	NS	16.2 (0.94)	12.8 (0.76)
P-3B, 9	near-surface plume; N = 93, N_{HC} = 55	0.45 (0.49)	12.6 (0.94)	0.035 (0.92)	0.083 (0.81)	0.049 (0.89)	7.56 (0.94)	−0.66 (0.69)	14.0 (0.46)	17.4 (0.57)
DC-8, 4	below ~4 km; N = 86; N_{HC} = 87	0.89 (0.79)	12.0 (0.72)	0.045 (0.93)	0.13 (0.89)	0.085 (0.92)	8.92 (0.92)	−0.90 (0.56)	11.45 (0.65)	19.39 (0.80)
P-3B, 19	plume at 2.5–3.5 km; N = 61, N_{HC} = 37	0.21 (0.84)	10.2 (0.63)	0.038 (0.58)	0.060 (0.70)	0.095 (0.62)	8.75 (0.67)	0.50 (0.43)	39.3 (0.48)	3.72 (0.64)
	Average	0.55	13.1	0.046	0.119	0.12	8.49	0.04	22.5	11.54
	Standard Deviation	0.24	2.0	0.007	0.035	0.07	1.17	0.99	9.8	5.4
					W to SW Trajectories					
DC-8, 14	plume at higher altitude; N = 350, N_{HC} = 192	0.36 (0.39)	13.8 (0.39)	0.078 (0.67)	0.073 (0.33)	0.210 (0.44)	8.12 (0.50)	0.40 (0.21)	34.9 (0.80)	4.56 (0.65)
DC-8, 10	above ~4 km; N = 257, N_{HC} = 131	0.38 (0.48)	8.7 (0.37)	0.048 (0.40)	0.093 (0.42)	0.190 (0.42)	9.32 (0.42)	0.33 (0.41)	22.3 (0.75)	6.61 (0.83)
P-3B, 9	N = 267, N_{HC} = 117	0.22 (0.69)	12.8 (0.81)	0.043 (0.82)	0.052 (0.66)	0.148 (0.82)	7.47 (0.62)	0.38 (0.59)	51.9 (0.90)	5.55 (0.89)
DC-8, 4	plume 4–~10 km; N = 148, N_{HC} = 161	0.41 (0.85)	13.0 (0.83)	0.052 (0.98)	0.082 (0.88)	0.154 (0.82)	7.57 (0.74)	0.51 (0.60)	27.6 (0.78)	7.69 (0.85)
DC-8, 18	plume above 6 km; N = 210, N_{HC} = 124	0.35 (0.74)	12.4 (0.76)	0.063 (0.68)	0.094 (0.68)	0.22 (0.46)	11.3 (0.60)	0.51 (0.54)	34.3 (0.95)	4.88 (0.76)
P-3B, 6	plume at 3 km; N = 171, N_{HC} = 88	0.33 (0.72)	19.4 (0.41)	0.064 (0.52)	0.086 (0.67)	0.212 (0.21)	10.71 (0.37)	0.44 (0.63)	66.8 (0.73)	3.97 (0.74)
DC-8, 12	narrow well-defined layer;N = 14, N_{HC} = 13	0.43 (0.97)	28.1 (0.99)	0.057 (0.98)	0.075 (0.95)	0.258 (0.97)	16.5 (0.91)	0.84 (0.91)	64.0 (0.96)	7.41 (0.96)
	Average	0.35	15.4	0.058	0.079	0.199	10.14	0.49	43.1	5.81
	Standard Deviation	0.07	6.4	0.012	0.014	0.039	3.18	0.17	17.8	1.45
					Clean/Aged					
P-3B, 9	tropical; N = 102, N_{HC} = 33	0.22 (0.20)	NS	NS	NS	NS	NS	NS	NS	3.94 (0.45)
P-3B, 6	generally low altitude; N = 126, N_{HC} = 65	1.29 (0.64)	30.2 (0.37)	0.136 (0.40)	0.228 (0.11)	0.481 (0.24)	29.9 (0.47)	−1.07 (0.11)	15.5 (0.26)	5.68 (0.52)

[a]Slopes ($\Delta y/\Delta x$) and coefficients of determination (r^2). Variables are given as y:x. Correlations below the 95% significance level are denoted as NS (not significant). Number of data points used in a regression are given as N for regressions of CH_4 with CO or CO_2 and N_{HC} for regressions with halocarbons and other hydrocarbons. Predominant transport pathways are based on 5 day back-trajectories [*Fuelberg et al.*, 2003].

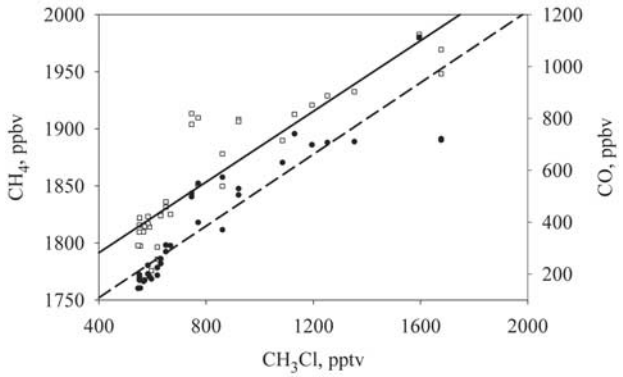

Figure 11. Shanghai plume, DC-8 Flight 13. Open squares: CH_4; Closed circles: CO. For regression lines: $\Delta CH_4/\Delta CH_3Cl = 0.154$, $r^2 = 0.81$; $\Delta CO/\Delta CH_3Cl = 0.69$, $r^2 = 0.85$.

Africa (Table 2). These plumes tended to be at higher altitudes and had enhanced mixing ratios of CH_3Cl, CO, and C_2H_2 as compared with those with trajectories to the northwest. In these air masses, CH_4 mixing ratios were highly correlated with both C_2Cl_4 and CH_3Cl and had generally lower $\Delta CH_4/\Delta CO$ values, within the range of those due to combustion [*Andreae and Merlet*, 2001]. The trace gas characteristics of these plumes are consistent with African, north Indian, and southeastern Asian source regions derived from back-trajectories. The relationship between CH_4 and C_2H_6 displays relatively little variability between plumes and/or transport pathways (Table 2), suggesting that emission ratios from the dominant sources of fossil fuel usage and biomass burning at this time are relatively constant. Similarity in source emission ratios may in part account for the very high correlation between the two gases observed throughout the region.

[29] On several TRACE-P flights, plumes with both types of transport pathways were sampled, illustrating the complex mix of emissions in Asian outflow. During DC-8 flight 10 in the vicinity of Hong Kong, outflow with back-trajectories to the northwest and with elevated C_2Cl_4, CO, CH_4, and other hydrocarbons was observed below approximately 4 km (Figure 12). Over the course of the flight, the aircraft repeatedly intercepted this air mass as a series of spirals were performed. Methane mixing ratios averaged 1818 ppbv, ranged up to 1883 ppbv, and were well correlated with a variety of trace gases with anthropogenic sources (Table 2). Above about 4 km, levels of CH_3Cl were elevated (Figure 12), and back-trajectories indicate that this relatively well-aged air passed across southeast Asia and regions to the west as far as India and Africa. Average C_2H_2/CO and C_3H_8/C_2H_6 values in this air mass were significantly lower than those below 4 km (1.58 versus 2.67 pptv/ppbv and 0.12 versus 0.29, respectively), suggesting that greater atmospheric processing (both photochemical and mixing) had occurred than in the air below 4 km. The slope of CH_3Cl relative to CO ($\Delta CH_3Cl/\Delta CO$) above 4 km is 0.95 pptv/ppbv ($r^2 = 0.69$), consistent with biomass burning values with a significant smoldering component [*Andreae et al.*, 1996; *Blake et al.*, 1996]. Although the correlation is also statistically significant, the $\Delta CH_3Cl/\Delta CO$ slope in the near-surface air mass is much lower (0.26 pptv/ppbv; $r^2 = 0.67$). Consistent with the lower CH_3Cl inputs in near-surface air, the calculated $\Delta CH_4/\Delta CH_3Cl$ is higher than in air above 4 km (1.20 ppbv/pptv; $r^2 = 0.43$, as compared with 0.33; $r^2 = 0.41$), even though $\Delta CH_4/\Delta CO$ values are quite similar (Table 2).

[30] At higher altitudes during the P-3B flight 9 in the Hong Kong area, the aircraft intercepted air of largely tropical origin at several locations, with low trace gas mixing ratios (mean CO = 77 ppbv; CH_4 = 1746 ppbv; $C_2H_2/CO = 0.92$). Close to the surface, an air mass with high C_2Cl_4 but very little CH_3Cl was sampled that had 5-day trajectories extending back to the north and west over China and into Siberia (Figure 13a). This layer was characterized by elevated CO, CH_4, and other hydrocarbons (mean CH_4 = 1822 ppbv; C_2H_6 = 1877 pptv; C_2Cl_4 = 8.9 pptv; CH_3Cl = 569 pptv; and $C_3H_8/C_2H_6 = 0.29$). The majority of the air sampled during the flight was polluted with a complex mixture of urban/industrial and combustion sources with source trajectories generally from the west and southwest. Both C_2Cl_4 and CH_3Cl were enhanced (averaging 4.7 and 630 pptv, respectively), as were a suite of trace gases, and C_3H_8/C_2H_6 ratios averaged 0.14, suggesting that at least several days had elapsed since emission (Figure 13b).

[31] During the P-3B transit flight 6 from Kona, Hawaii (19.7°N, 156.0°W) to Wake Island (19.32°N, 166.6°E) on 27 February, an extremely thin, well-defined polluted layer was noted at approximately 3 km. The aircraft intercepted this layer repeatedly over the entire flight path, suggesting that it was present over a large geographic region. This air mass

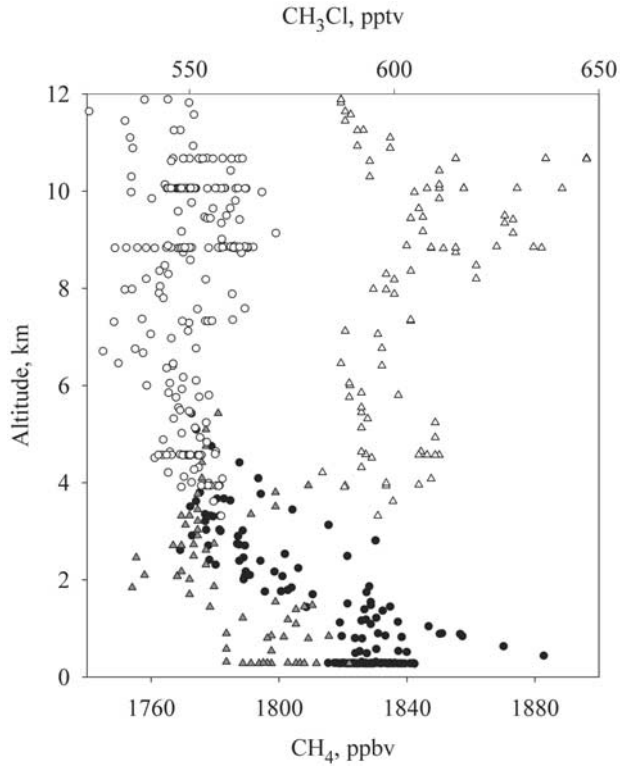

Figure 12. Methane mixing ratios during DC-8, Flight 10. For CH_4: (open circles) above ~4 km; (solid circles) below ~4 km. For CH_3Cl: (open triangles) above ~4 km; (grey triangles) below ~4 km.

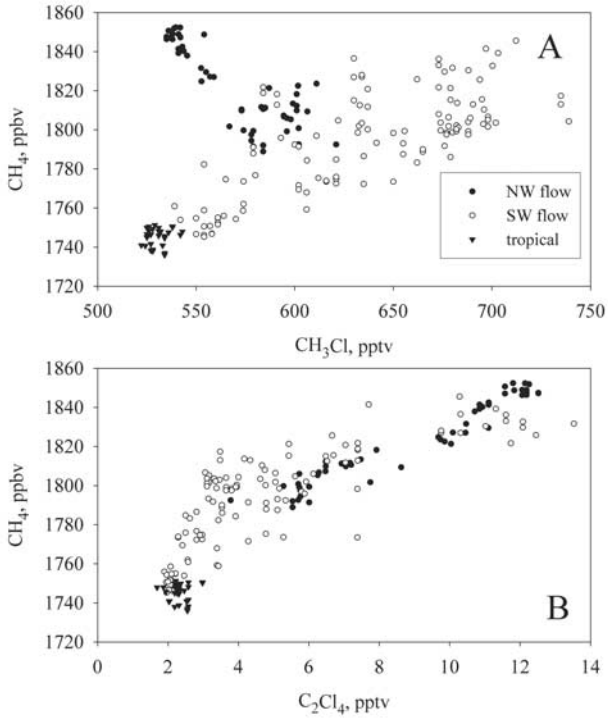

Figure 13. Methane mixing ratios for air masses sampled during P-3B Flight 9. (a) CH_4 and CH_3Cl; (b) CH_4 and C_2Cl_4. Solid triangles: Air with tropical trajectories; Solid circles: Near-surface plume with northwest back-trajectories; Open circles: Air with southwest back-trajectories.

was characterized by enhanced levels of both CH_3Cl (averaging 623 pptv) and C_2Cl_4 (averaging 5.1 pptv; Figure 14), and had 5 day back trajectories extending back over Japan and into China. The calculated $\Delta CH_4/\Delta CO$ for this air mass is 0.33, indicative of combustion inputs with characteristically low emission ratios. At altitudes of 5–6 km, the maximum altitude sampled by the aircraft, relatively clean air with largely tropical oceanic back trajectories was observed, with low CO (average = 84 ppbv), CH_4 (average = 1693 ppbv), and other trace gases (Figure 14a). Dominating the near-surface altitudes sampled and mixing into the relatively clean air is an air mass with apparently few combustion inputs (Figure 14b). Five-day back trajectories for much of this relatively well-aged air suggests that it had been over water for this time, with some flows extending to the east, towards the North American continent. The calculated $\Delta CH_4/\Delta CO$ for this air mass is 1.29, and is consistent with urban emission ratios (Table 2). The slope for the relationship between CH_4 and C_2H_6 is unusually high as compared to others seen during the mission (0.14 ppbv/pptv; Table 2) and the correlation between the two gases, as well as that between CH_4 and other hydrocarbons, is unusually low, indicating a well aged air mass that has lost these shorter-lived gases.

4. Changes in CH_4 With Time: Comparison With PEM-West B

[32] Part of the rationale behind the TRACE-P mission was to compare measurements over this region with those made 7 years earlier during PEM-West B (PWB) and to assess any basin-wide changes as industrialization has proceeded on the Asian continent [*Jacobs et al.*, 2003]. Because a major objective of both the TRACE-P and PWB missions was to sample and characterize polluted continental outflow to the Pacific, we expect trace gas mixing ratios to be elevated well above background levels. Since this objective was common to both missions, they should share a similar sampling bias and comparisons between missions should be possible. As shown in Figure 15, it is clear that significantly different CH_4 mixing ratios were sampled during the two missions. Despite the overall change in concentrations and sparser geographic coverage however, latitudinal and longitudinal trends similar to those discussed for TRACE-P are apparent in Figure 15 for PWB.

4.1. Trends With Latitude

[33] In the Western Pacific below 2 km, TRACE-P mixing ratios average 21 ± 16 ppbv above CMDL background latitudinal means. For PWB, using seasonally weighted average CH_4 mixing ratios for CMDL Pacific sites, calculated as for those in section 3.1 for TRACE-P, this difference was comparable, 26 ± 19 ppbv. Enhancement over background levels is minimal south of 15°N during TRACE-P and relatively constant north of 15°N, ranging between 27 and 38 ppbv (Figure 5a). Differences between latitude means and background levels were somewhat different for PWB than for TRACE-P. Elevated mixing

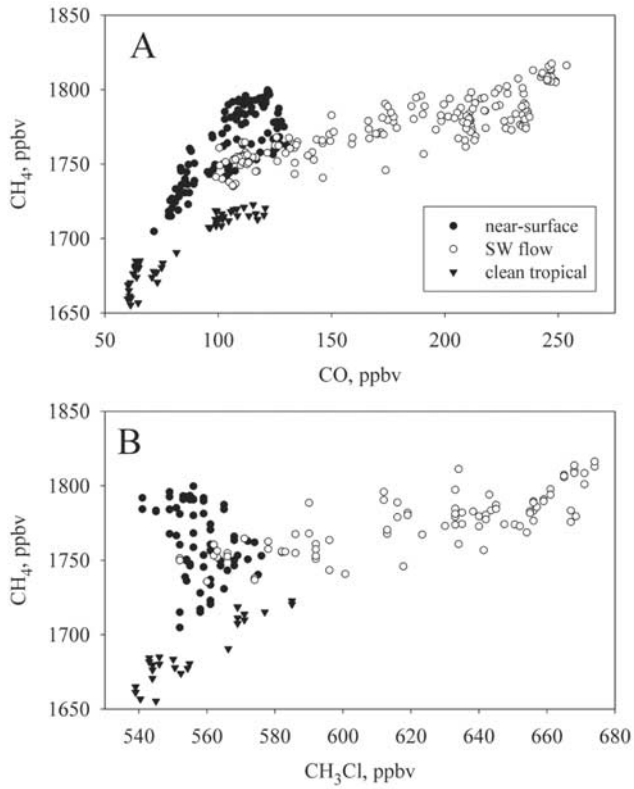

Figure 14. Methane mixing ratios for air masses sampled during P-3B Flight 6. (a) CH_4 and CO; (b) CH_4 and CH_3Cl. Solid triangles: Tropical oceanic trajectories; Open circles: plume at 3 km with southwest back-trajectories; Solid circles: near-surface Asian outflow.

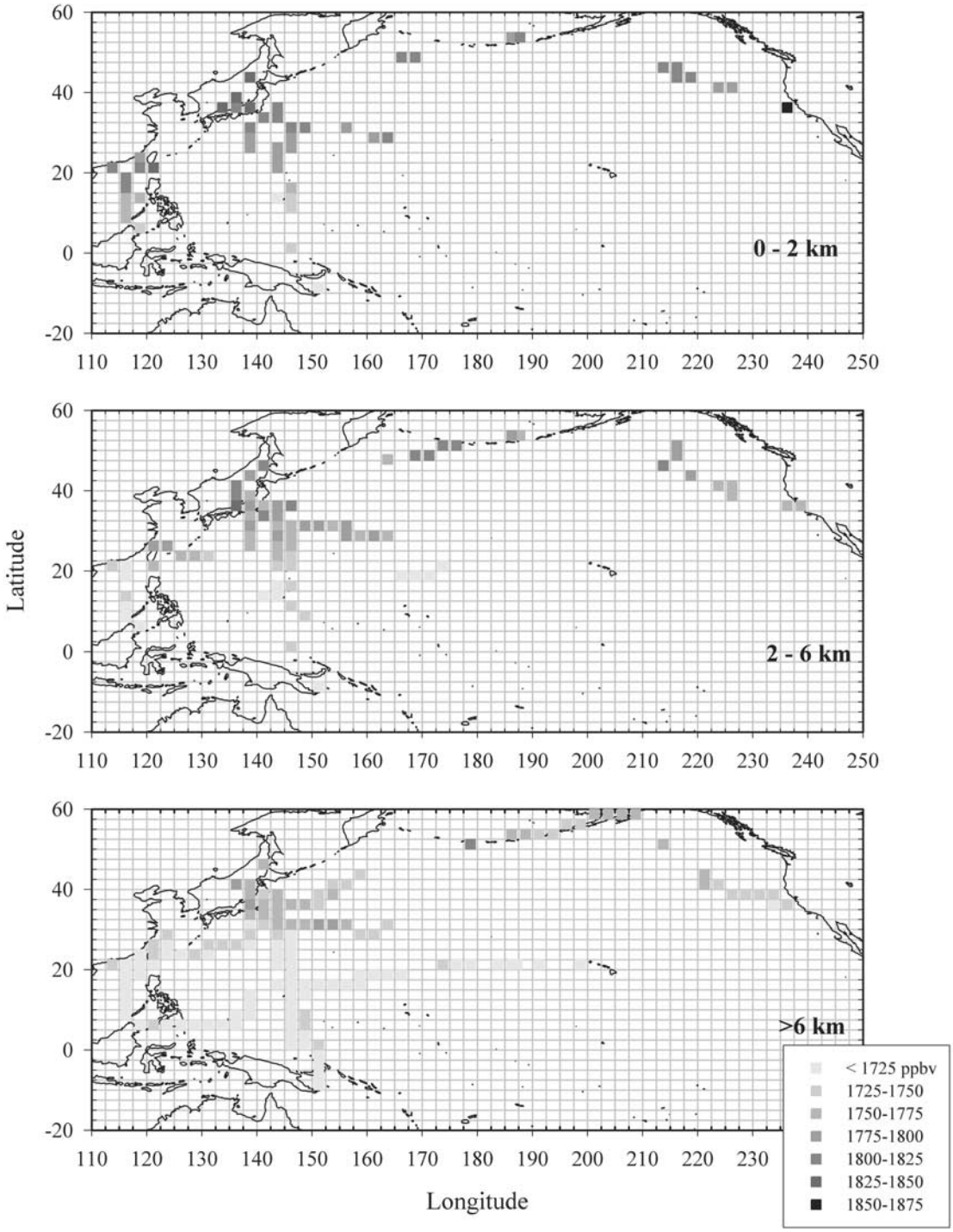

Figure 15. Regional distribution of CH_4 during PEM-West B, as for Figure 2. See color version of this figure at back of this issue.

ratios were sharply higher between 15 and 25°N, fell somewhat, then increased more gradually with increasing latitude north. Maximum enhancement over background levels was 57 ppbv between 20 and 25°N. Rather than the broad region of higher concentrations seen during TRACE-P, elevated CH_4 levels were focused in a more restricted area. The average enhancement over CMDL background levels north of 15°N is similar however between the missions; 31 ± 5 ppbv during TRACE-P and 32 ± 20 ppbv during PWB. Between 5 and 15°N, little enhancement over CMDL levels is seen for TRACE-P (0.2 ± 0.1 ppbv). It was greater during PWB, averaging 14 ± 10 ppbv. At Central/Eastern longitudes, average differences between mission and CMDL latitudinal means are 5 ± 6 and 16 ± 13 ppbv for TRACE-P and PWB respectively, suggesting that enhancements over background were roughly similar during the two missions.

[34] Figure 16 compares latitudinal trends in CH_4 for the two missions in both the Western Pacific and Central/

Eastern Pacific. Comparisons between missions are best for the Western Pacific where data for both missions were collected more intensely and there is greater temporal and spatial overlap. On average in the near-surface at these longitudes, CH_4 mixing ratios during TRACE-P are 27 ± 12 ppbv greater than those of PWB, ranging from 11 to 47 ppbv. The smallest difference is observed between the latitudes of 20 and 25°N where CH_4 inputs were high during PWB and the greatest enhancement over CMDL clean air levels were seen. Average near-surface differences between missions for other hydrocarbons are negative, with PWB mixing ratios higher than those for TRACE-P; by 209 ± 311 pptv for C_2H_6, 138 ± 235 pptv for C_2H_2, and 222 ± 275 pptv for C_3H_8.

[35] Latitudinal trends for CH_4 and C_2H_6 (Figures 17a–17c) and CH_3Cl and C_2Cl_4 (Figures 17d–17f) in the West Pacific for the two missions illustrate some of the similarities between the missions. Near-surface ethane levels at latitudes south of 20°N appear to be quite similar while greater mixing ratios between 20 and 25°N and north of 35°N are observed during PWB (Figure 17a). Although many of the objectives of the expeditions were similar, they were not identical and the execution of objectives varied so that differences may reflect any sampling bias between the missions. However, because TRACE-P was flown several weeks later in the spring than PWB, seasonal changes in OH, the major atmospheric sink, would be expected to result in lower background levels of the shorter-lived NMHCs. This effect should be greatest in the lower troposphere and in the northern hemisphere, where seasonal variability is highest. Differences in the latitudinal distribution of C_2H_6 (Figure 17a) as well as C_2H_2 and C_3H_8 (data not shown), are consistent with this explanation and suggest that the spring seasonal decrease in NMHCs likely contributes to between-mission differences.

[36] Mixing ratios of C_2Cl_4 are also strikingly higher in the near-surface of PWB, by an average of 11 ± 7 pptv, while those for CH_3Cl are not significantly different, differing by an average of only 2 ± 33 pptv (Figure 17d). Above the boundary layer, (Figures 17e and 17f), average PWB C_2Cl_4 levels are also greater than those of TRACE-P, although average differences are smaller than those below 2 km. Differences in mixing ratios of CH_3Cl remain variable and overall, not significantly different. Although these differences may suggest that PWB observed greater industrial inputs in the region than during TRACE-P and comparable combustion inputs, significant differences in the usage of C_2Cl_4 occurred between the two missions, accounting for at least part of this change [*McCulloch et al.*, 1999; *U.S. Environmental Protection Agency*, 1994; *Schettler et al.*, 1999]. *McCulloch et al.* [1999] calculate a global decrease in industrial emissions of C_2Cl_4 of 0.023 ± 0.10 Tg/yr between 1988 and 1996, 6% of the baseline 1990 emissions from this source. The change in latitudinal distribution above the boundary layer (Figure 17e and17f) would suggest that the decrease in northern hemisphere C_2Cl_4 sources is the most likely explanation for differences between missions.

[37] Latitudinal CH_4 means in the free troposphere (2–6 km; Figure 17b) are on average 29 ± 9 ppbv higher for TRACE-P, similar to the difference seen in near-surface values. At these altitudes, the greatest differences are observed south of 25°N. Above 6 km (Figure 16c), CH_4 differences were somewhat greater, by 39 ± 12 ppbv. As seen in Figure 17, average CH_4 and C_2H_6 mixing ratios within the Western Pacific are highly correlated for both missions.

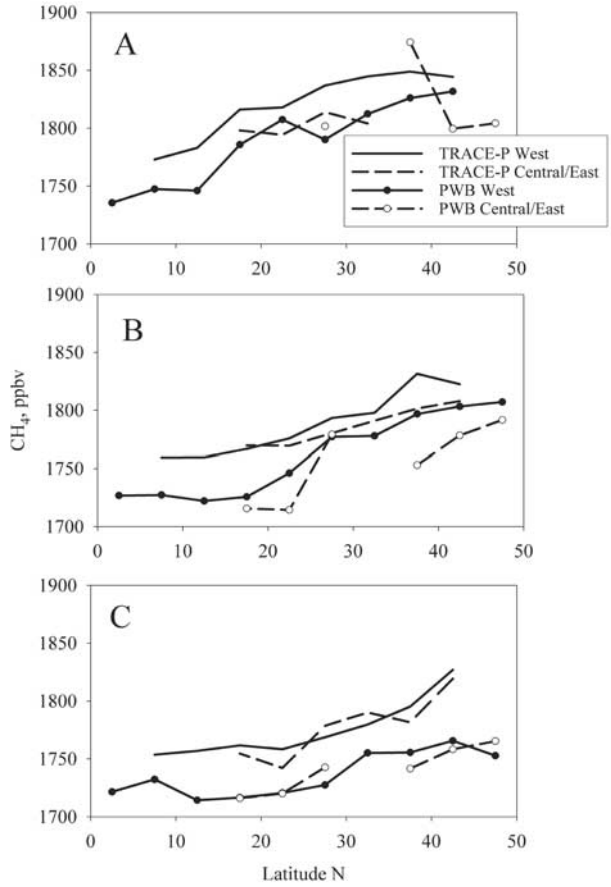

Figure 16. Latitudinal CH_4 trends by longitude class and altitude for PEM-West B and TRACE-P. (a) 0–2 km; (b) 2–6 km; and (c) >6 km.

4.2. Trends With Altitude

[38] As shown in Figure 18, average altitude profiles during PWB for CH_4 and a variety of other hydrocarbons appear to be quite similar to those seen in TRACE-P (Figure 10) and the high correlation between CH_4 and these gases was also present during the mission ($\Delta CH_4/\Delta CO$ = 0.74, r^2 = 0.79; $\Delta CH_4/\Delta C_2H_6$ = 0.046 ppbv/pptv, r^2 = 0.91; $\Delta CH_4/\Delta C_2Cl_4$, = 4.56 ppbv/pptv, r^2 = 0.85). Although quite similar, the relationship between CH_4 and C_2H_6 is significantly different than that calculated for TRACE-P (0.050) at the 95% confidence level. The PWB regression slopes for CH_4 and CO and for CH_4 and C_2Cl_4 differ at the 99% level. The regression slope of CH_4 with CO is steeper in PWB (0.74 versus 0.58 for TRACE-P) and that with C_2Cl_4 is shallower (4.56 versus 7.37 ppbv/pptv for TRACE-P). The latter is likely a reflection of the significantly higher C_2Cl_4 inputs during PWB. *Liu et al.* [2003] suggest that convection over Southeast Asia may have been enhanced during TRACE-P relative to PWB. A greater contribution from

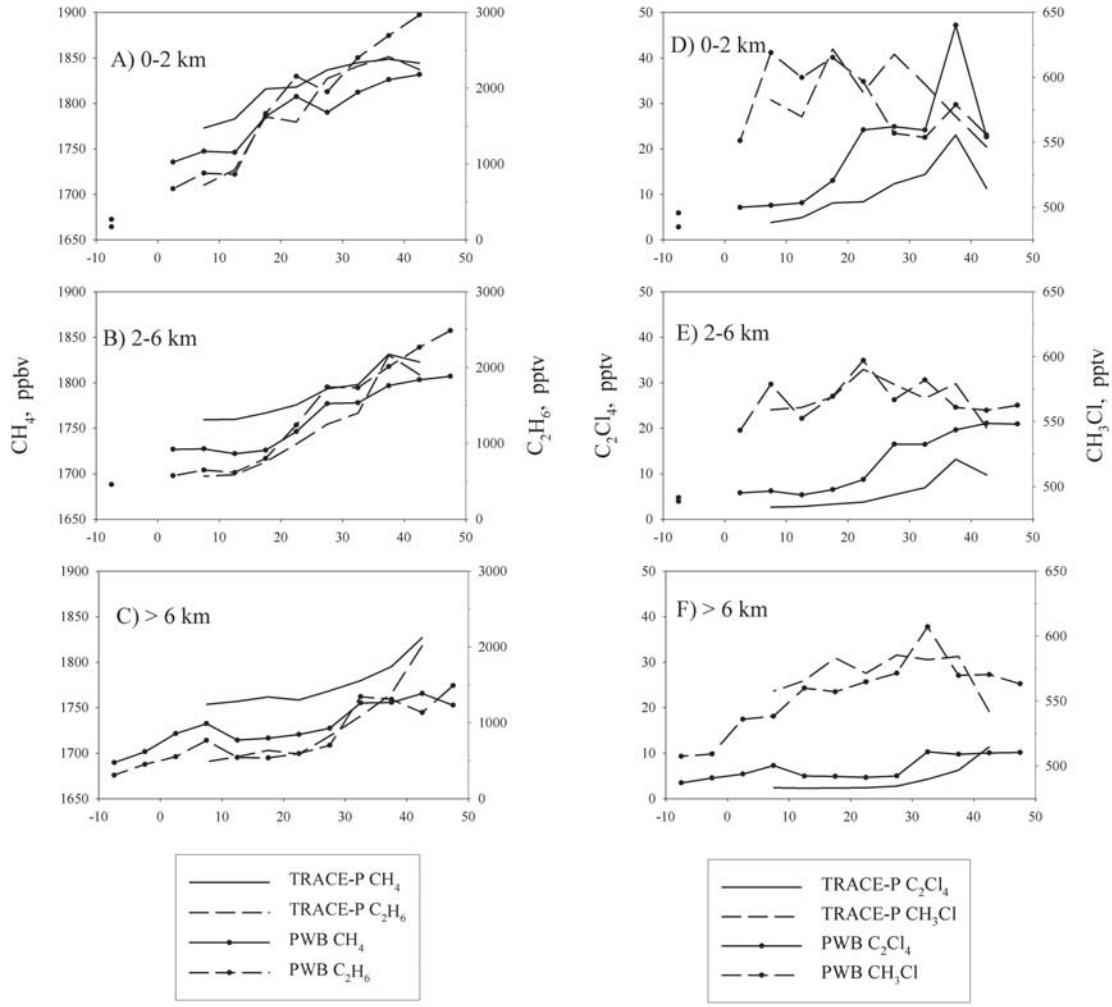

Figure 17. Latitudinal trends with altitude in the Western Pacific (west of 160°E) during TRACE-P and PWB. For CH_4 and C_2H_6: (a) 0–2 km; (b) 2–6 km; and (c) >6 km. For perchloroethene (C_2Cl_4) and methyl chloride (CH_3Cl): (d) 0–2 km; (e) 2–6 km; and (f) >6 km.

biomass burning in this region as well as changes in Asian sources between the missions may contribute to the different relationship between CH_4 and CO.

4.3. Regional Comparisons

[39] Figures 2 and 15 highlight the significant difference in overall CH_4 levels observed across the Pacific Basin over a 7 year time interval. These differences however, include contributions from any seasonal disparities between the mission and changes in the global background levels, as well as any possible meteorological variability and source changes. In order to examine any air quality changes due to industrialization and land use change, we must account for these other contributions.

[40] Although TRACE-P and PWB were conducted at roughly the same time of year, the several week offset could be a concern for CH_4 as well as the NMHCs, since it has a significant seasonal cycle. Monthly averages based on CMDL Pacific background air samples (Figure 19a) suggest that this source of variability is relatively small for CH_4 but that the increase over the 7 years between the missions is large. Although there can be significant longitudinal variability in CH_4, as shown above in section 4.3, longitudinal variability in background levels for a long-lived trace gas such as CH_4 is much smaller than that due to differences in the latitudinal distribution of sources [*Dlugokencky et al.*, 1994]. Comparison of CMDL background latitudinal means for the two missions (Figure 19b), indicates a relatively constant difference between the PWB and TRACE-P time periods over the domain of most interest between 10°N and 40°N. Latitudinal variability in background differences may in part be due to differential growth in source types. Between 50°S and 30°N, differences in CMDL background levels range from 12 to 55 ppbv and average 41 ± 7 (1 σ). Similar calculations for background sites outside of the Pacific basin yield comparable differences (data not shown). Using all the CMDL sites, we derive a global background difference of 38 ± 6 ppbv for latitudes south of 30°N between the two missions. North of 30°N, average differences are 25 ± 10 ppbv (Pacific) and 29 ± 14 ppbv (non-Pacific), yielding a global average of 27 ± 12 ppbv. Although lower latitude sites in the Pacific Basin tend to

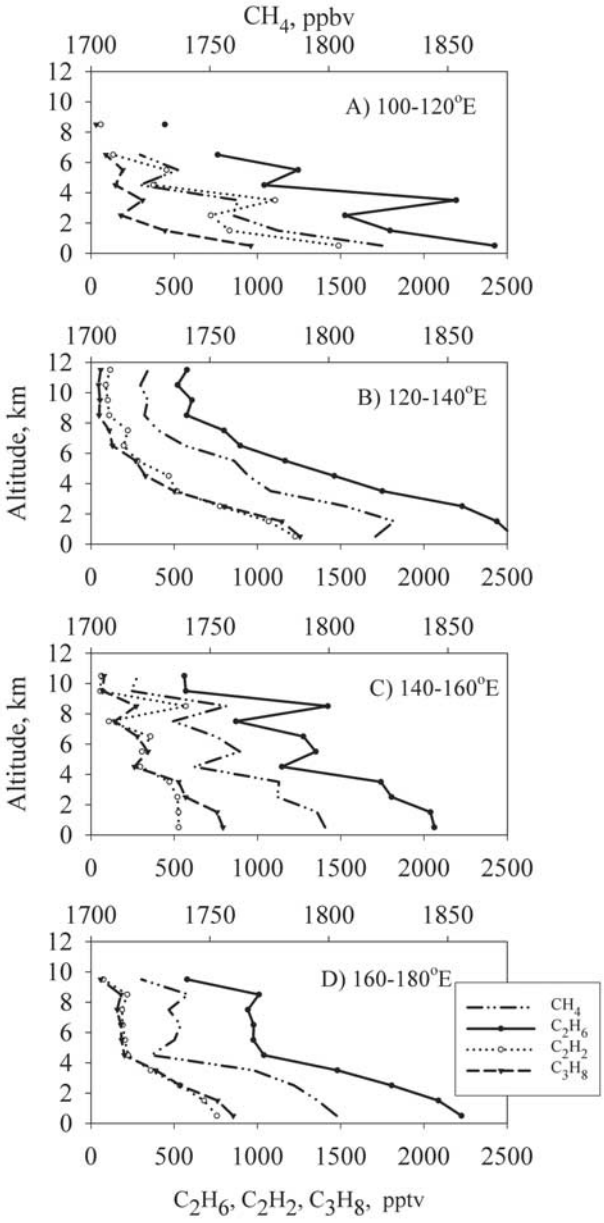

Figure 18. PEM-West B average altitude profiles for CH_4 and selected hydrocarbons, 20°N–40°N; 20° longitude classes; as for Figure 10 for TRACE-P. (a) 100–120°E; (b) 120–140°E; (c) 140–160°E; and (d) 160–180°E.

have slightly higher differences between missions, suggesting perhaps that sources may have increased there more than in other regions, these differences are not statistically significant.

[41] Assuming that the meteorological setting of the two missions is roughly similar, as indicated by *Fuelberg et al.* [2003], and that transport of continental outflows were comparably sampled, calculations based on the observed changes in background mixing ratios suggest that the average changes in CH_4 seen between missions, on the order of 30–40 ppbv (section 5.1), are likely to be primarily a result of an increasing background rather than a change in emissions due to changing land use and/or industrialization. Although our CMDL reference background concentrations are sampled at the surface, because CH_4 is a long-lived gas, upper altitude concentrations should reflect those at surface-level since rates of mixing are rapid relative to photochemical loss. This assumption seems reasonable since differences between missions above the boundary level are similar to those within it. The high correlation observed for both missions between CH_4 and other hydrocarbons such as C_2H_6, may however, provide an additional way to examine the change in CH_4 at all altitudes between the two missions since the NMHCs are not thought to have significant long-term background trends due to shorter atmospheric lifetimes.

[42] In Figure 20, we show the correlation between differences in CH_4 and C_2H_6 between PWB and TRACE-P for highly averaged spatial data. The data used to calculate differences are 1 km altitude means for six large geographic regions, the broad latitude and longitude classes discussed previously (south of 20°N, 20–40°N, north of 40°N and either east or west of 160°E). As shown in Figures 10 and 18 and discussed above, variability in CH_4 and C_2H_6 between PWB and TRACE-P are highly correlated. Based on this relationship and the assumption that there is relatively little long-term change in C_2H_6 in comparison to CH_4 [*Rinsland et al.*, 2000; *Zhao et al.*, 2002], the y-intercept yields an estimate of the change in CH_4 between the missions. This calculation is complicated however, by the seasonal cycle in C_2H_6 and the offset in timing between the two missions.

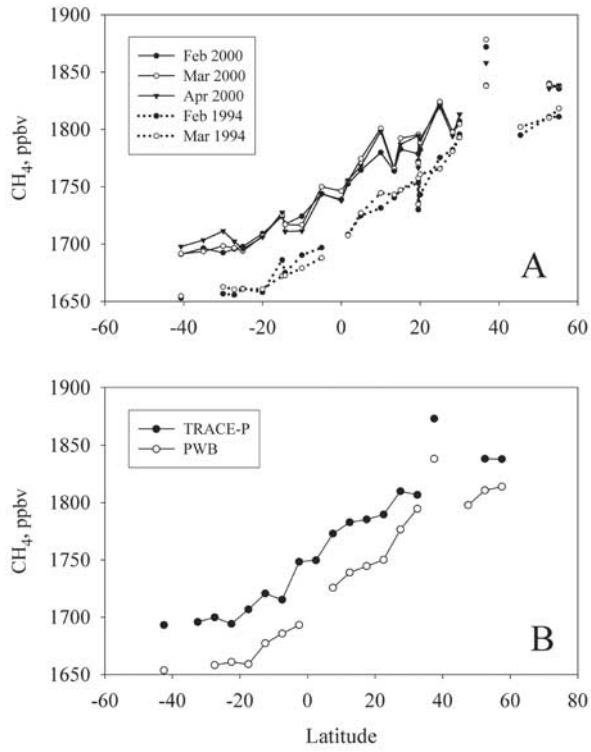

Figure 19. (a) Monthly average CH_4 mixing ratios for Pacific Basin CMDL sites during the PEM-West B and TRACE-P missions, by latitude. Elevated values at 36.7°N are for the Tae-ahn Peninsula, Korea, known to have high CH_4 levels. (b) As for Figure 19a, but averaged for the duration of the missions and grouped into 5° latitude classes.

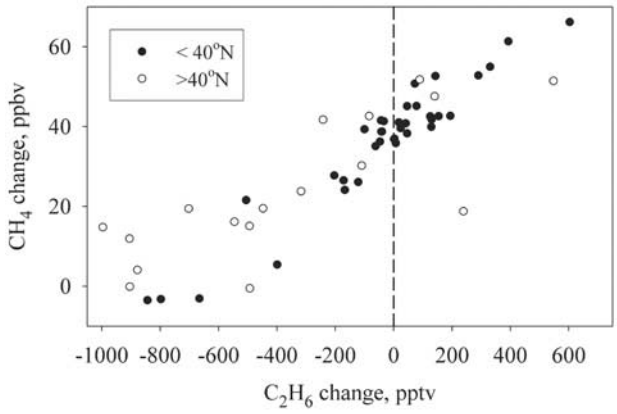

Figure 20. Differences in spatially averaged CH_4 and C_2H_6 mixing ratios between PEM-West B and TRACE-P. Data are 1 km altitude averages for three latitude classes (north of 40°N, 20°N–40°N, south of 20°N) and two longitude classes (west of 160°E and east of 160°E). Open circles: North of 40°N; solid circles: South of 40°N.

Seasonal variability in C_2H_6 is greatest in the lower altitudes of the high northern latitudes [*Rudolph*, 1995; *Gupta et al.*, 1998], a function both of greater seasonal changes in the atmospheric OH sink in the north and the latitudinal distribution of sources. Here, we can partially compensate for the seasonal cycle and the several week offset between the missions by only using data from the <20°N and 20–40°N latitude classes. Restricting the data in Figure 20 in this way demonstrates that much of the variability in C_2H_6 decrease between missions (PWB higher than TRACE-P) occurs north of 40°N. The largest of these negative values are observed at altitudes below 3 km. The correlation between changes in CH_4 and C_2H_6 yields a change "offset" for CH_4 of 38 ppbv ($r^2 = 0.92$). Inclusion of higher latitude data decreases the coefficient of determination but results in little alteration in the calculated intercept because the relationship for all of the data is driven largely by the lower latitude values.

[43] Dispersion along the regression line in Figure 20 is an indirect measure of spatial variability between the missions, since we would expect points to form a cluster at 0 change for C_2H_6 and roughly 38 ppbv for CH_4 if transport and geographic regions were perfectly paired. Note that for C_2H_6, positive and negative mission differences are roughly equal and average a nonsignificant -41 ± 296 pptv, indicating that there was relatively little sampling bias, such as a disproportionate sampling of plumes, between the missions. These calculations of course, shed little light on any effects of sampling bias on the regional representativeness of the observations. Similar calculations for changes between missions in CH_4 and C_2H_2 and CH_4 and C_3H_8 yield comparable "change offsets" of 36 ppbv ($r^2 = 0.81$, $\Delta CH_4/\Delta C_2H_2 = 0.089$ ppbv/pptv, n = 37) and 41 ppbv ($r^2 = 0.84$, $\Delta CH_4/\Delta C_3H_8 = 0.097$ ppbv/pptv, n = 37) respectively.

[44] Correlations between changes between missions in CH_4 and other trace gases such as CO can also be calculated. For CO, the relationship between the two is not as strong, in part because major sources such as combustion and fossil fuel use vary in their CH_4/CO ratios. Differences between missions yield a "change offset" for CH_4 of 29 ppbv ($r^2 = 0.55$, n = 53, $\Delta CH_4/\Delta CO = 0.45$), lower than calculated with the hydrocarbons, again suggesting that either the relative mix of sources may be different between the two missions, as discussed in section 5.3, or that the assumption of little to no long-term change in CO is invalid. Spectroscopic and tropospheric measurements indicate that CO concentrations have either decreased somewhat [*Novelli et al.*, 1998; *Zhao et al.*, 2002] or remained relatively constant [*Rinsland et al.*, 2000] over the last decade. As a consequence of its relatively short atmospheric lifetime, changes in CO sources and sinks are reflected rapidly in its interannual trends. Increasing trends prior to about 1990 may have been the result of industrialization while recent decreases may be due to decreases in biomass burning [*Novelli et al.*, 1998]. Restricting the data to latitudes south of 40°N improves the correlation between CH_4 and CO (CH_4 offset = 31 ppbv, $r^2 = 0.70$, n = 39, $\Delta CH_4/\Delta CO = 0.58$), probably due to latitudinal differences in the CO seasonal cycle as for C_2H_6. Restricting the relationship to latitudes below 40°N may also change the relative mix between types of sources, as indicated by a shift in regression slope from 0.45 to 0.58. Calculations using changes in C_2H_2/CO ratios and CH_4 yield values in agreement with those using hydrocarbons.

[45] Agreement between the various hydrocarbons for estimating a basin-wide mission difference in CH_4 is excellent and their consistency with the calculated background change derived from CMDL surface data both confirms the assumption that there is little long-term change in the NMHCs as well as the conclusion that changes in Asian industrialization and land use over the last 7 years are not reflected in obvious additional changes in levels of CH_4 throughout the air column. Given the relatively long atmospheric lifetime of CH_4 this may not be an unexpected finding since changes in emissions are integrated into background levels and the response time of atmospheric mixing ratios to changes in emissions is fairly rapid [see, e.g., *Tans*, 1997].

5. Summary

[46] The high-resolution, high-precision CH_4 data set collected during TRACE-P during the north Asian spring highlights the importance of continental outflow to the North Pacific Basin at this time. Trace gas ratios ($\Delta CH_4/\Delta CO$) and source-specific tracers such as C_2Cl_4 for urban/industrial sources and CH_3Cl for combustion indicate that these outflows are complex mixtures of trace gases from a variety of sources that are rapidly carried into the basin by the strong westerly transport characteristic of this time of year [*Fuelberg et al.*, 2003]. Five-day trajectories calculated for elevated trace gases in plume layers suggest that sources as far upwind as Africa, India, Southeast Asia, and Siberia make contributions to the pollution observed during the mission. Trajectories from the southwest and west (Africa, India, Southeast Asia) carry trace gas signatures indicating higher inputs from combustion sources than those from the northwest (Siberia, northern China). Overall, the high correlations between spatially averaged CH_4 mixing ratios and those of C_2H_6 and other hydrocarbons, as well as C_2Cl_4, indicate that urban/industrial sources dominate regional inputs. Comparisons between TRACE-P and PEM-West B, flown during roughly the same time of year and

under a similar meteorological setting 7 years earlier, suggest that although the TRACE-P CH_4 observations are significantly higher, changes in CH_4 largely parallel those seen in background air over this time interval. Although clearly significant changes in population, land use, and industrialization have occurred between the two missions, these comparisons would imply that any regional emission changes are difficult to isolate from those upwind and are not reflected in basin-wide changes in CH_4 levels over and above the changes already included in the baseline rise of this long-lived trace gas.

[47] **Acknowledgments.** This work was made possible by support from the NASA GTE program and we wish to thank the GTE staff, led by Vickie Connors, for their help. Excellent logistical support on this complex expedition was provided by the pilots, missions managers, and crew of the Wallops P-3B and the Dryden DC-8 aircraft. We greatly appreciate use of data on background levels of CH_4, provided courtesy of Ed Dlugokencky and the Climate Monitoring and Diagnostic Laboratory (CMDL). We appreciate the thoughtful comments of Nicola Blake on an earlier manuscript version as well as those of three anonymous reviewers.

References

Andreae, M. O., and P. Merlet, Emission of trace gases and aerosols from biomass burning, *Global Biogeochem. Cycles*, *15*, 955–966, 2001.

Andreae, M. O., et al., Methyl halide emissions from savanna fires in southern Africa, *J. Geophys. Res.*, *101*, 23,603–23,613, 1996.

Bartlett, K. B., G. W. Sachse, J. E. Collins Jr., and R. C. Harriss, Methane in the tropical South Atlantic: Sources and distribution during the late dry season, *J. Geophys. Res.*, *101*, 24,139–24,150, 1996.

Bey, I., D. J. Jacob, J. A. Logan, and R. M. Yantosca, Asian chemical outflow to the Pacific in spring: Origins, pathways, and budgets, *J. Geophys. Res.*, *106*, 23,097–23,113, 2001.

Blake, D. R., and F. S. Rowland, Continuing world-wide increase in tropospheric methane, 1978–1987, *Science*, *239*, 1129–1131, 1988.

Blake, N. J., D. R. Blake, B. C. Sive, T.-Y. Chen, F. S. Rowland, J. E. Collins Jr., G. W. Sachse, and B. E. Anderson, Biomass burning emissions and vertical distribution of atmospheric methyl halides and other reduced carbon gases in the South Atlantic region, *J. Geophys. Res.*, *101*, 24,151–25,164, 1996.

Blake, N. J., D. R. Blake, T.-Y. Chen, J. E. Collins Jr., G. W. Sachse, B. E. Anderson, and F. S. Rowland, Distribution and seasonality of selected hydrocarbons and halocarbons over the western Pacific basin during PEM-West A and PEM-West B, *J. Geophys. Res.*, *102*, 28,315–28,331, 1997.

Blake, N. J., et al., Large-scale latitudinal and vertical distribution of NMHCs and selected halocarbons in the troposphere over the Pacific Ocean during the March–April 1999 Pacific Exploratory Mission (PEM - Tropics B), *J. Geophys. Res.*, *106*, 32,627–32,644, 2001.

Blake, N. J., et al., NMHCs and halocarbons in Asian continental outflow during TRACE-P: Comparison to PEM-West B, *J. Geophys. Res.*, *108*(D20), 8806, doi:10.1029/2002JD003367, in press, 2003.

Bräunlich, M., O. Aballain, T. Marik, P. Jöckel, C. A. M. Brenninkmeijer, J. Chappellaz, J.-M. Barnola, R. Mulvaney, and W. T. Sturges, Changes in the global atmospheric methane budget over the last decades inferred from ^{13}C and D isotopic analysis of Antarctic firn air, *J. Geophys. Res.*, *106*, 20,465–20,481, 2001.

Brocard, D., J.-P. Lacaux, and H. Eva, Domestic biomass combustion and associated atmospheric emissions in West Africa, *Global Biogeochem. Cycles*, *12*, 127–139, 1998.

Browell, E. V., et al., Large-scale ozone and aerosol distributions, air mass characterics, and ozone fluxes over the western Pacific Ocean in the late-winter/early-spring, *J. Geophys. Res.*, *108*(D20), 8805, doi:10.1029/2002JD003290, in press, 2003.

Cooke, W. F., B. Koffi, and J.-M. Grégoire, Seasonality of vegetation fires in Africa from remote sensing data and application to a global chemistry model, *J. Geophys. Res.*, *101*, 21,051–21,065, 1996.

Dlugokencky, E. J., L. P. Steele, P. M. Lang, and K. A. Masarie, The growth rate and distribution of atmospheric methane, *J. Geophys. Res.*, *99*, 17,021–17,043, 1994.

Dlugokencky, E. J., K. A. Masarie, P. M. Lang, and P. P. Tans, Continuing decline in the growth rate of the atmospheric methane burden, *Nature*, *393*, 447–450, 1998.

Ehhalt, D. H., F. Rohrer, A. B. Knaus, M. J. Prather, D. R. Blake, and F. S. Rowland, On the significance of regional trace gas distributions as dervived from aircraft campaigns in PEM-West A and B, *J. Geophys. Res.*, *102*, 28,333–28,351, 1997.

Eisele, F. L., et al., Summary of measurement intercomparisons during TRACE-P, *J. Geophys. Res.*, *108*(D20), 8791, doi:10.1029/2002JD003167, in press, 2003.

Etheridge, D. M., L. P. Steele, R. J. Francey, and R. L. Langenfelds, Atmospheric methane between 1000 A.D. and present: Evidence of anthropogenic emissions and climatic variability, *J. Geophys. Res.*, *103*, 15,979–15,993, 1998.

Ferek, R. J., J. S. Reid, P. V. Hobbs, D. R. Blake, and C. Liousse, Emission factors of hydrocarbons, halocarbons, trace gases and particles from biomass burning in Brazil, *J. Geophys. Res.*, *103*, 32,107–32,118, 1998.

Francey, R. J., M. R. Manning, C. E. Allison, S. A. Coram, D. M. Etheridge, R. L. Langenfelds, D. C. Lowe, and L. P. Steele, A history of $\delta^{13}C$ in atmospheric CH_4 from the Cape Grim air archive and Antarctic firn air, *J. Geophys. Res.*, *104*, 23,631–23,643, 1999.

Fuelberg, H. E., C. M. Kiley, J. R. Hannan, D. J. Westberg, M. A. Avery, and R. E. Newell, Atmospheric transport during the Transport and Chemical Evolution over the Pacific (TRACE-P) experiment, *J. Geophys. Res.*, *108*(D0), 8782, doi:10.1029/2002JD003092, in press, 2003.

Gupta, M., S. Tyler, and R. Cicerone, Modeling atmospheric $\delta^{13}CH_4$ and the causes of recent changes in atmospheric CH_4 amounts, *J. Geophys. Res.*, *101*, 22,923–22,932, 1996.

Gupta, M. L., R. J. Cicerone, D. R. Blake, F. S. Rowland, and I. S. A. Isaksen, Global atmospheric distributions and source strenths of light hydrocarbons and tetrachloroethene, *J. Geophys. Res.*, *103*, 28,219–28,235, 1998.

Hao, W. M., and M.-H. Liu, Spatial and temporal distribution of tropical biomass burning, *Global Biogeochem. Cycles*, *8*, 495–503, 1994.

Harris, J. M., E. J. Dlugokencky, S. J. Oltmans, P. P. Tans, T. J. Conway, P. C. Novelli, K. W. Thoning, and J. D. W. Kahl, An interpretation of trace gas correlations during Barrow, Alaska, winter dark periods, 1986–1997, *J. Geophys. Res.*, *105*, 17,267–17,278, 2000.

Harriss, R. C., G. W. Sachse, J. E. Collins Jr., L. Wade, K. B. Bartlett, R. W. Talbot, E. V. Browell, L. A. Barrie, G. F. Hill, and L. G. Burney, Carbon monoxide and methane over Canada: July–August 1990, *J. Geophys. Res.*, *99*, 1659–1669, 1994.

Heald, C. L., D. J. Jacob, P. I. Palmer, M. Evans, G. Sachse, D. Blake, and H. Singh, Biomass burning emission inventory with daily resolution: Application to aircraft observations of Asian outflow, *J. Geophys. Res.*, *108*(D21), 8811, doi:10.1029/2002JD003082, in press, 2003.

Hoell, J. M., D. D. Davis, S. C. Liu, R. E. Newell, H. Akimoto, R. J. McNeal, and R. J. Bendura, The Pacific Exploratory Mission-West Phase B: February–March 1994, *J. Geophys. Res.*, *102*, 28,223–28,239, 1997.

Houweling, S., F. Dentener, and J. Lelieveld, The modeling of tropospheric methane: How well can point measurements be reproduced by a global model?, *J. Geophys. Res.*, *105*, 8981–9002, 2000.

Jacob, D. J., J. H. Crawford, M. M. Kleb, V. E. Connors, R. J. Bendura, J. L. Raper, G. W. Sachse, J. C. Gille, L. Emmons, and C. L. Heald, The Transport and Chemical Evolution over the Pacific (TRACE-P) aircraft mission: Design, execution, and first results, *J. Geophys. Res.*, *108*(D20), 8781, doi:10.1029/2002JD003276, in press, 2003.

Khalil, M. A. K., R. A. Rasmussen, M. J. Shearer, R. W. Dalluge, L. Ren, and C.-L. Duan, Factors affecting methane emissions from rice fields, *J. Geophys. Res.*, *103*, 25,219–25,231, 1998.

Lelieveld, J., et al., The Indian Ocean Experiment: Widespread pollution from South and Southeast Asia, *Science*, *291*, 1031–1036, 2001.

Liu, H., D. J. Jacob, I. Bey, R. M. Yantosca, B. N. Duncan, and G. W. Sachse, Transport pathways for Asian combustion outflow over the Pacific: Interannual and seasonal variations, *J. Geophys. Res.*, *108*(D20), 8786, doi:10.1029/2002JD003102, in press, 2003.

Lobert, J. M., D. H. Scharffe, W.-M. Hao, T. A. Kuhlbusch, R. Seuwen, P. Warneck, and P. J. Crutzen, Experimental evaluation of biomass burning emissions: Nitrogen and carbon containing compounds, in *Global Biomass Burning-Atmospheric, Climatic, and Biospheric Implications*, edited by J. S. Levine, MIT Press, Cambridge, Mass., 1991.

Matthews, E., I. Fung, and J. Lerner, Methane emission from rice cultivation: Geographic and seasonal distribution of cultivated areas and emissions, *Global Biogeochem. Cycles*, *5*, 3–24, 1991.

McCulloch, A., M. L. Aucott, T. E. Graedel, G. Kleiman, P. M. Midgley, and Y.-F. Li, Industrial emissions of trichloroethene, tetrachloroethene, and dichloromethane: Reactive Chlorine Emissions Inventory, *J. Geophys. Res.*, *104*, 8417–8428, 1999.

McKeen, S. A., S. C. Liu, E.-Y. Hsie, X. Lin, J. D. Bradshaw, S. Smyth, G. L. Gregory, and D. R. Blake, Hydrocarbon ratios during PEM-West A: A model perspective, *J. Geophys. Res.*, *101*, 2087–2109, 1996.

Merrill, J. T., R. E. Newell, and A. S. Bachmeier, A meteorological overview for the Pacific Exploratory Mission-West Phase B, *J. Geophys. Res.*, *102*, 28,241–28,253, 1997.

Novelli, P. C., K. A. Masarie, and P. M. Lang, Distributions and recent changes of carbon monoxide in the lower troposphere, *J. Geophys. Res.*, *103*, 19,015–19,033, 1998.

Parrish, D. D., C. J. Hahn, E. J. Williams, R. B. Norton, F. C. Fehsenfeld, H. B. Singh, J. D. Shetter, B. W. Gandrud, and B. A. Ridley, Indications of photochemical histories of Pacific air masses from measurements of atmospheric trace species at Point Arena, California, *J. Geophys. Res.*, *97*, 15,883–15,902, 1992.

Prinn, R. G., R. F. Weiss, B. R. Miller, J. Huang, F. N. Alyea, D. M. Cunnold, P. J. Fraser, D. E. Hartley, and P. G. Simmons, Atmospheric trends and lifetimes of CH_3CCl_3 and global OH concentrations, *Science*, *269*, 187–192, 1995.

Randriambelo, T., J.-L. Baray, and S. Baldy, Effect of biomass burning, convective venting, and transport on tropospheric ozone over the Indian Ocean: Reunion Island field observations, *J. Geophys. Res.*, *105*, 11,813–11,832, 2000.

Rasmussen, R. A., L. E. Rasmussen, M. A. K. Khalil, and R. W. Dalluge, Concentration distribution of methyl chloride in the atmosphere, *J. Geophys. Res.*, *85*, 7350–7356, 1980.

Rinsland, C. P., et al., Northern and southern hemisphere ground-based infrared spectroscopic measurements of tropospheric carbon monoxide and ethane, *J. Geophys. Res.*, *103*, 28,197–28,217, 1998.

Rinsland, C. P., E. Mahieu, R. Zander, P. Demoulin, J. Forrer, and B. Buchmann, Free tropospheric CO, C_2H_6, and HCN above central Europe: Recent measurements from the Jungfraujoch station including the detection of elevated columns during 1998, *J. Geophys. Res.*, *105*, 24,235–24,249, 2000.

Rudolph, J., The tropospheric distribution and budget of ethane, *J. Geophys. Res.*, *100*, 11,369–11,381, 1995.

Sachse, G. W., G. F. Hill, L. O. Wade, and M. G. Perry, Fast-response, high-precision carbon monoxide sensor using a tunable diode laser absorption technique, *J. Geophys. Res.*, *92*, 2071–2081, 1987.

Sachse, G. W., J. E. Collins, G. F. Hill, L. O. Wade, L. G. Burney, and J. A. Ritter, Airborne tunable diode laser sensor for high precision concentration and flux measurements of carbon monoxide and methane, *Proc. SPIE Int. Opt. Eng.*, *1433*, 145–156, 1991.

Schettler, T., G. Solomon, M. Valenti, and A. Huddle, *Generations at Risk: Reproductive Health and the Environment*, 417 pp., MIT Press, Cambridge, Mass., 1999.

Scholes, R. J., D. E. Ward, and C. O. Justice, Emission of trace gases and aerosol particles due to vegetation burning in southern hemisphere Africa, *J. Geophys. Res.*, *101*, 23,677–23,682, 1996.

Smyth, S., et al., Comparison of free tropospheric western Pacific air mass classification schemes for the PEM-West A experiment, *J. Geophys. Res.*, *101*, 1743–1762, 1996.

Streets, D. G., K. Jiang, X. Hu, J. E. Sinton, X.-Q. Zhang, D. Xu, M. Z. Jacobson, and J. E. Hansen, Recent reductions in China's greenhouse gas emissions, *Science*, *294*, 1835–1837, 2001.

Streets, D. G., et al., An inventory of gaseous and primary aerosol emissions in Asia in the year 2000, *J. Geophys. Res.*, *108*(D21), 8809, doi:10.1029/2002JD003093, in press, 2003.

Talbot, R. W., et al., Chemical characteristics of continental outflow from Asia to the troposphere over the western Pacific Ocean during February–March 1994: Results from PEM-West B, *J. Geophys. Res.*, *102*, 28,255–28,274, 1997.

Tans, P. P., A note on isotopic ratios and the global atmospheric methane budget, *Global Biogeochem. Cycles*, *11*, 77–81, 1997.

U. S. Environmental Protection Agency, Chemicals in the environment: Perchloroethylene, *CAS 127-18-4*, Washington, D. C., 1994.

Wang, C. J.-L., D. R. Blake, and R. S. Rowland, Seasonal variations in the atmospheric distribution of a reactive chlorine compound, tetrachloroethene ($CCl_2 = CCl_2$), *Geophys. Res. Lett.*, *22*, 1097–1100, 1995.

Wild, O., J. K. Sundet, M. J. Prather, I. S. A. Isaksen, H. Akimoto, E. V. Browell, and S. J. Oltmans, CTM ozone simulations for spring 2001 over the western Pacific: Comparisons with TRACE-P lidar, ozonesondes, and TOMS columns, *J. Geophys. Res.*, *108*(D21), 8826, doi:10.1029/2002JD00328, in press, 2003.

Yao, H., Y.-H. Zhuang, and Z. L. Chen, Estimation of methane emissions from rice paddies in mainland China, *Global Biogeochem. Cycles*, *10*, 641–649, 1996.

Zhao, Y., K. Strong, Y. Kondo, M. Koike, Y. Matsumi, H. Inrie, C. P. Rinsland, N. B. Jones, K. Suzuki, H. Nakajima, H. Nakane, and I. Murata, Spectroscopic measurements of tropospheric CO, C_2H_6, C_2H_2, and HCN in northern Japan, *J. Geophys. Res.*, *107*(D18), 4343, doi:10.1029/2001JD000748, 2002.

K. B. Bartlett, Complex Systems Research Center, University of New Hampshire, Morse Hall, Durham, NH 03824, USA. (karen@kaos.sr.unh.edu)

D. R. Blake, Department of Chemistry, University of California, Irvine, Irvine, CA 92697, USA. (drblake@uci.edu)

C. Harward, Science Applications International Corporation, c/o NASA Langley Research Center, MS 468, Hampton, VA 23681, USA. (c.n.harward@larc.nasa.gov)

G. W. Sachse, NASA Langley Research Center, Hampton, VA 23681, USA. (g.w.sachse@larc.nasa.gov)

T. Slate, Swales Aerospace, c/o NASA Langley Research Center, MS 468, Hampton, VA 23681, USA. (t.a.slate@larc.nasa.gov)

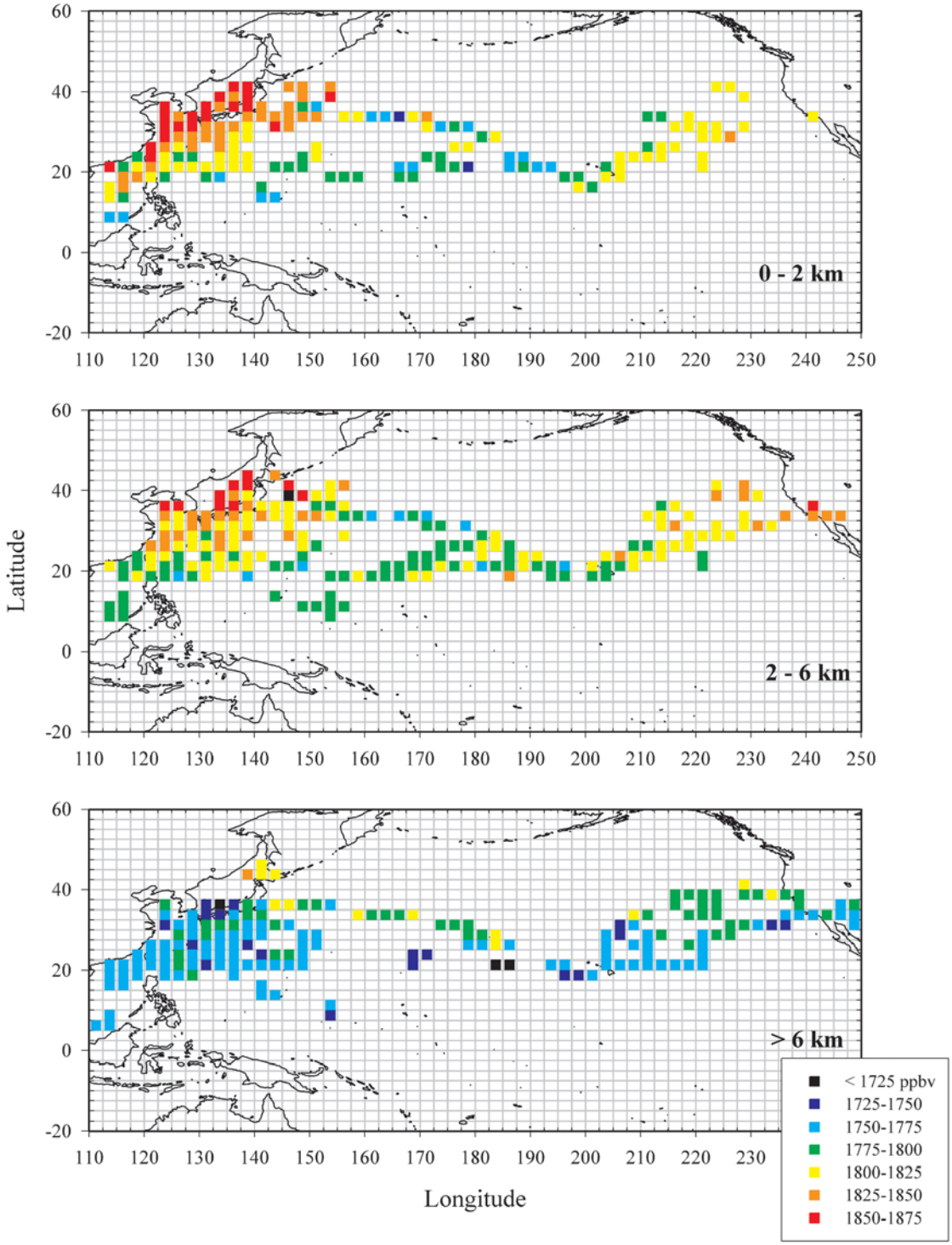

Figure 2. Regional distribution of CH_4 during the TRACE-P expedition; 0–2 km, 2–6 km, and above 6 km. Data were grouped into 2.5° latitude × 2.5° longitude areas then averaged. Number of observations within areas vary.

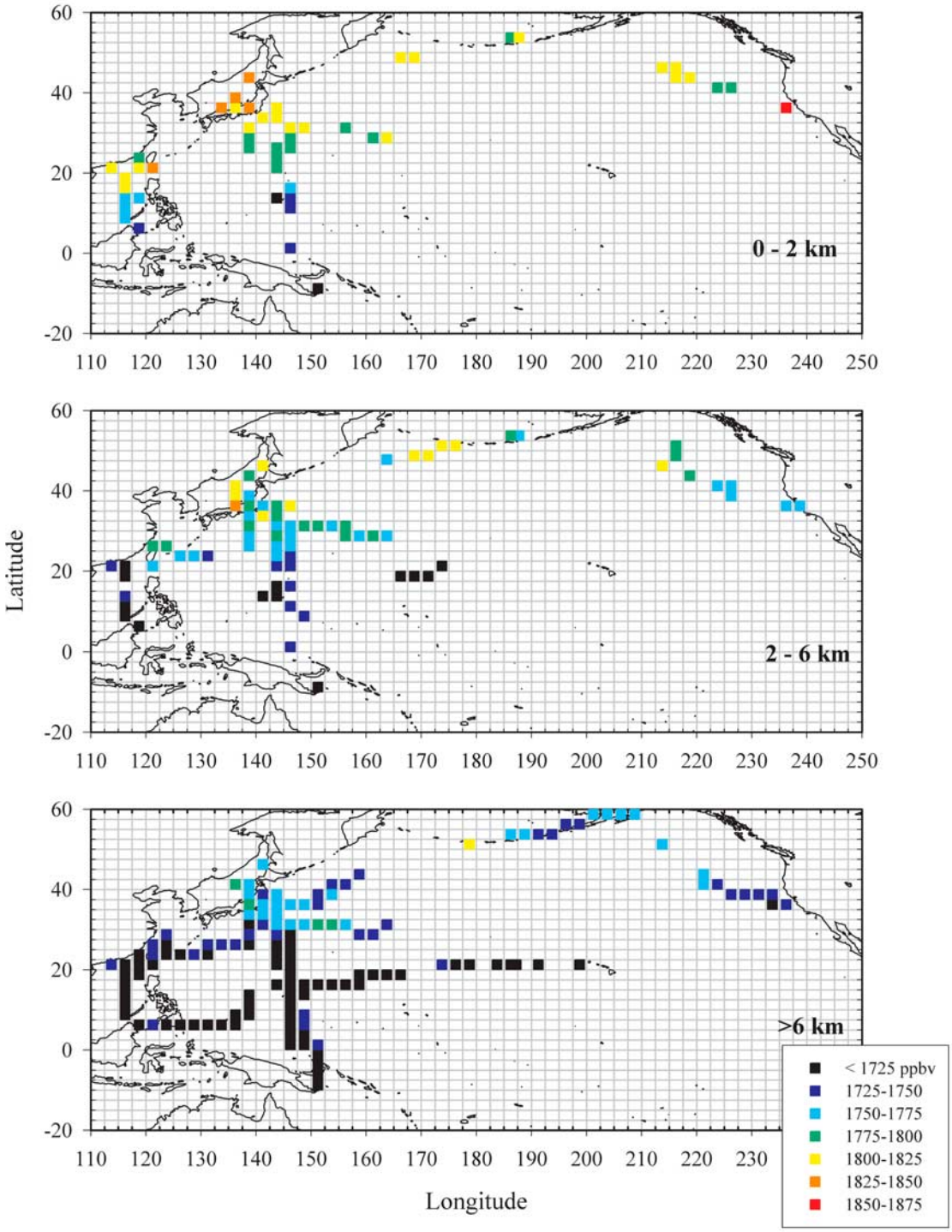

Figure 15. Regional distribution of CH_4 during PEM-West B, as for Figure 2.